The Uppermost Nappes in the Asterousia Mountains - Gerokampos to Agios Kyrillos

View of the marble cliffs on the way to Agios Kyrillos from Gerokampos. The mountains consist predominantly of metapelite, which has been intruded by diorite magma and minor granitoid veins. The mountain in the middle of the picture displays large marble bodies. The various rocks on this route also include serpentinites, indicating obduction of oceanic crust. On the whole the rocks are highly metamorphic and partly display migmatite textures.

Compiled by George Lindemann, MSc.

Berlin, August 2024

Content

Appendix

1 Introduction

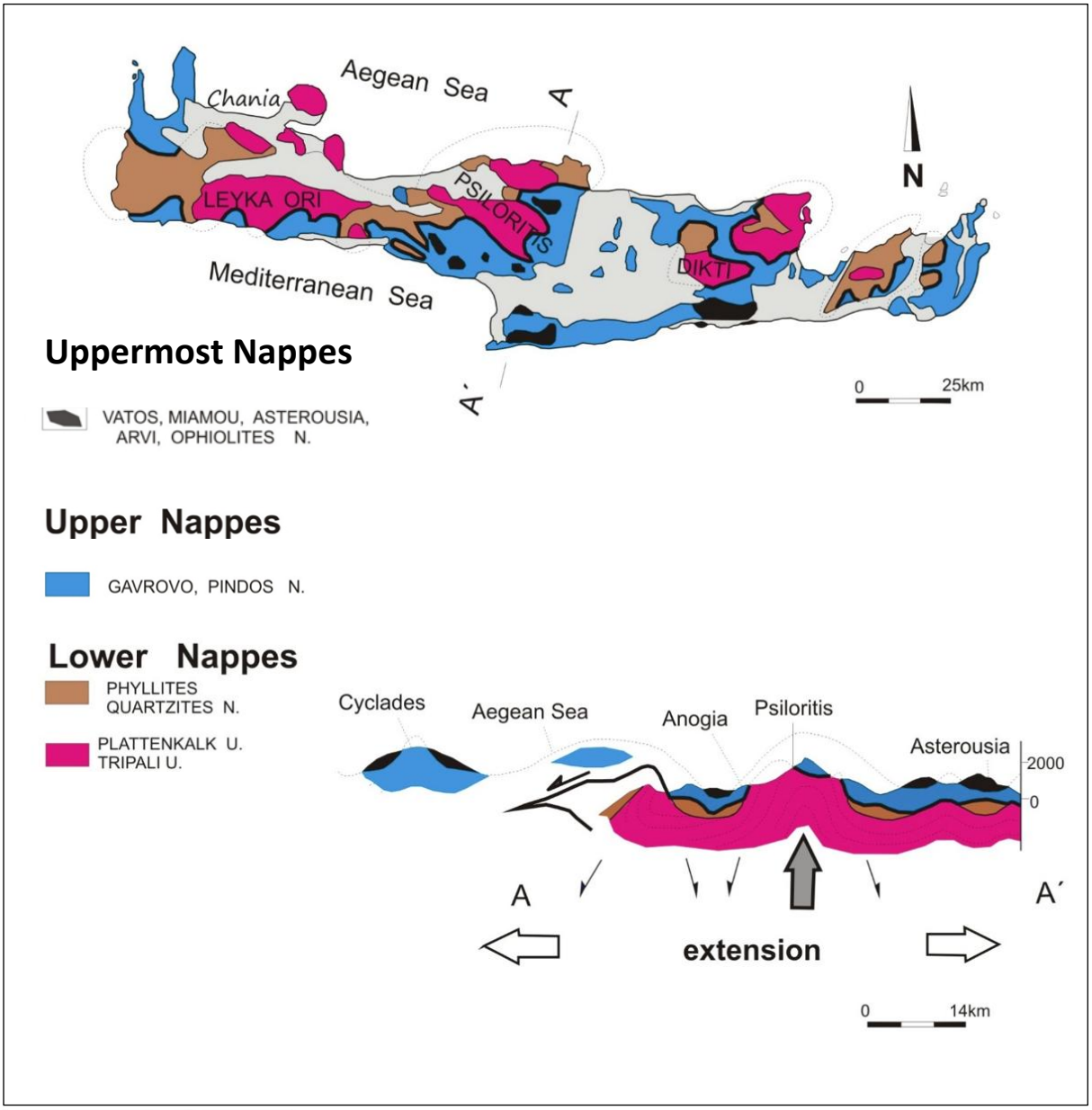

Source: Journal of the virtual explorer (NW Crete, online), slightly modified
https://virtualexplorer.com.au/article/2011/285/neotectonic-study-of-western-crete/setting.html

A nappe or thrust sheet is a large sheetlike body of rock that has been moved several tens or even hundreds of kilometers along a thrust plane from its original position. Nappes form in convergent tectonic settings such as continental collision zones or on the overriding plate in active subduction zones. The resulting structure may include large-scale recumbent folds, shearing along the fault planes, imbricate thrust stacks, fensters and klippes *[Wikipedia]*.

A characteristic feature of the Uppermost Nappes of southern and central Crete is the frequent occurrence of ophiolites, which represent pieces of oceanic crust predominantly from ocean ridges. Ophiolites consist of mafic to ultramafic plutonic and volcanic rocks and often exhibit deep marine sediments such as clay (i.e. shale, slates and phyllites), chert and deep marine limestones. The ultramafic rock is often hydrothermally altered to serpentinite.

In central Crete, the ophiolite-bearing Uppermost Nappes feature tectonic mélanges that are indicated to be the result of chaotic thrusts within the accretionary wedge of a subduction zone (cf. Cowan, 1985; Hsu, 1968; Raymond, 1984). These assemblages of disrupted rocks represent the highest tectonic nappes overlying the Tripolitza and the Pindos Nappes. *[Tortorici]*

Recent work by Zulauf et. al. 2023 indicates that the Uppermost Nappes can be divided into several separate nappes, based on their lithology and on the grade and timing of metamorphism (e.g. Bonneau, 1972; Krahl, Herbart & Katzenberger, 1982; Tortorici et al. 2012). There are two different stacks one of which is exposed in central Crete near Plakias and the other in the Asterousia Mountains. The nappe stack in the Asterousia Mountains consists of the Avri, Miamou, "Green Schist" (mostly south of Dikti Mts.) and the Asterousia Crystalline Complex (see also My GeoGuide "No. 22 Uppermost Nappes within the Asterousia Mts., - Coast Road Kali Limenes to Chrysostoms" concerning the nappes along the coast) *[Zulauf]*.

The Amphibolite facies metamorphic rocks that are intruded by Late Cretaceous granitoid plutonic rocks (Kneuker et al. 2015; Martha et al. 2016, 2017) are referred to as the Asterousia Crystalline Complex (ACC), which is generally regarded to correlate with the southern margin of the Pelagonian domain and therefore lies within the Internal Hellenides (Martha et al. 2017). Other tectonometamorphic nappes ascribed to the Uppermost Unit include the Arvi Unit (prehnite-pumpellyite facies), which is interpreted as a Maastrichtian seamount at the northern margin of the Pindos realm (Palamakumbura, Robertson & Dixon, 2013), and the Greenschist Unit, consisting of fine-grained epidote-amphibole schist with a mid-ocean ridge basalt (MORB) -type signature (Reinecke et al. 1982; Martha et al. 2017) *[Martha]*. Note that not all of the nappes are exposed at or near at a single location owing to erosion and young sediment covering.

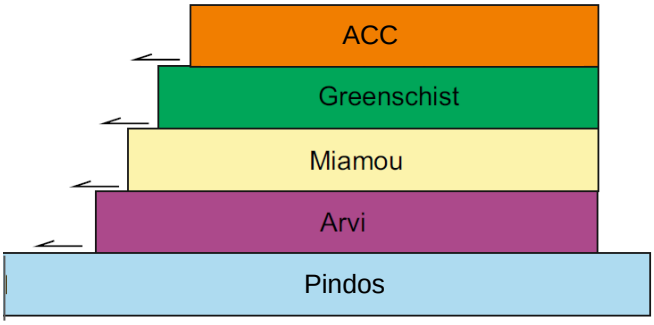

The Uppermost Nappes in the area of the Asteroussia Mountains (Zulauf et. al , 2023)

Unit/nappe Type	Protolith age	Metamorphic facies	Metamorphism Age
AC	?	Amphibolite-Granulite (2)	Campanian (2, 4, 5)
Greenschist	?	Greenschist (1, 4)	Paleocene (1)
Miamou	Kimmeridgian (15)	Greenschist (15)	?
Arvi	Upper Cretaceous (16, 17)	Prehnite-Pumpellyte (16, 17)	?

Reinecke et al. (1982), (2) Seidel et al. (1976), (3) Seidel et al. (1977), (4) Martha et al. (2017), (5) Martha et al. (2019), (6) Liati et al. (2004), (7) Bonneau and Lys (1978), (8) Zulauf et al. (2023a), (9) Koepke et al. (2002), (10) Malten (2019), (11) Koepke (1986), (12) Koepke et al. (1997), (13) Tortorici et al. (2012), (14) Zulauf et al. in prep., (15) Bonneau et al. (1974), (16) Robert and Bonneau (1982), (17) Palamakumbura et al. (2013), and (18) Karakitzios (1988)

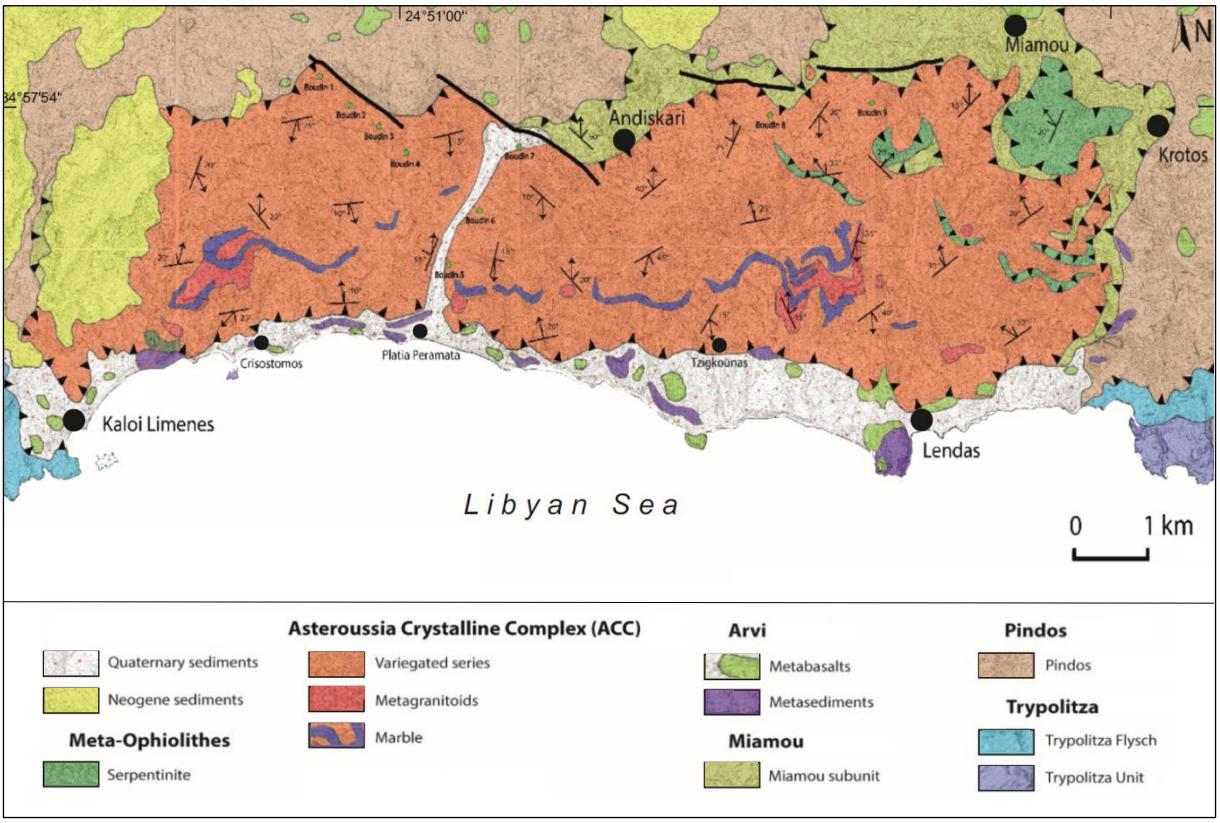

Geological map of the western part of the Asterousia Mountains showing the area between Kaloi Limenes and Lendas. Source: Zulauf G. et al., 2023, (modified after Davi and Bonneau 1972; Thorbecke 1987; Tortorici et al. 2012; Neuwirth 2018).

1.1 The Asteroussia nappe

The Asterousia Crystalline Complex (ACC) consists largely of high-grade metasedimentary rocks and occasional metagranitoids veins and sills (Langosch et al. 2000; Martha et al. 2019). In contrast to the other uppermost subnappes the ACC can be correlated with the southern margin of the Pelagonian domain and is therefore be associated with the Internal Hellinides realm (e.g. Aubouin & Dercourt, 1965; Bonneau, 1972; Martha et al. 2017). The ACC rocks consisting of amphibolite, quartzites, gneisses, and schists have undergone high-temperature/low-pressure metamorphism P = 400–500 MPa and Tmax = 700 °C (Seidel et al. 1981). Characteristic metamorphic minerals are sillimanite, andalousite, cordierite, hornblende, garnet and biotite, which denote an upper amphibolite facies. Existing slices of serpentinite are thought to have been incorporated into the metasedimentary rocks prior to amphibolite facies metamorphism (Bonneau 1973; Reinecke et al. 1982; Be'eri-Shlevin et al. 2009). *[Zulauf et al, 2023]*

During a short period in the middle to late Campanian (78–72 Ma) I-type granitoids were intruded into the metasedimentary succession. This is also the case on the island of Anafi, and on Crete near Melambes, and Pachia Amos (Kneuker et al. 2015; Martha et al. 2019). K–Ar biotite and hornblende ages of Cretan ACC-type rocks range from 76 to 66 Ma, while apatite fission-track ages of the ACC rocks near Lentas display ages of 31 to 20 Ma (Thomson et al. 1998) *[Zulauf, et. al., July 2023]*.

The geochemistry of the granitic intrusions (Langosch et al., 2000; Vandelli, 2010) indicates an arc (or fore-arc) related origin, which can be attributed to a subduction zone within the Pindos realm *[Stampfli]*.

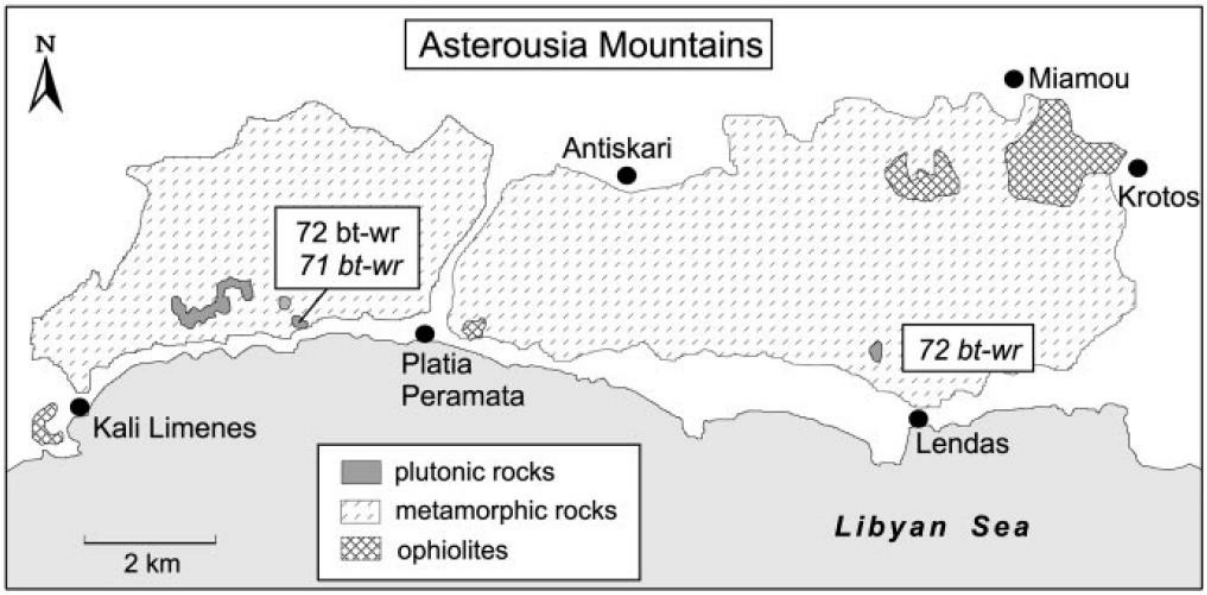

Sketch map of the outcrops of Late Cretaceous plutonic rocks in central Crete based on a map of the Asterousia Mountains after Davis and Bonneau (1985), with modifications. Only the crystalline rocks ophiolites are considered; other geological units are not specified (white areas). Numbers in boxes are Rb±Sr ages for biotite±whole-rock (bt-wr) or biotite±plagioclase±whole-rock (bt-pl-wr) and K±Ar ages for hornblende (hbl) or biotite (bt) in million years (for plutonic rocks shown in regular type, for paragneisses in italics). [Langosch A. et al. , 2000]

The largest occurrence of Late Cretaceous crystalline rocks is exposed in the Asterousia Mountains along the southern coast of central Crete, between the villages of Kali Limenes and Lendas (see sketch map above). *[Langosch A. et al. , 2000]*

Metamorphic assemblages, e.g. quartz-plagioclase-K-feldspar-sillimanite-biotite-garnet-cordierite in pelitic paragneisses, correspond to P-T conditions of the upper amphibolite facies, i.e. 650 to 700 °C and 4 to 6 kbar (Koepke and Seidel 1984). Locally, slices of lower-grade metamorphic rocks are intercalated with the high-T metamorphic sequence. The assemblage quartz-muscovite-chlorite-garnet-andalusite-plagioclase and quartz-muscovite-biotite-staurolite-andalusite-plagioclase, observed in metapelites of those slices, indicate metamorphic conditions of the lower amphibolite facies (550 °C, 3 kbar).

Intrusive rocks in the Asterousia Mountains are restricted to two relatively small areas. Mainly felsic granitoids are found in the hills 24 km east of Kali Limenes, while most of the more mafic rocks are exposed about 2 km NNW of Lendas close to the road from Gerokampos to Agios Kyrillos. The Asterousia plutonic rocks display a foliation which is mostly faint, but in some cases conspicuous. Frequently, the contacts between granitoids and the country rocks are sharp and obviously of intrusive origin. However, blurred contacts to migmatitic paragneisses occur as well, and there is apparently no clear distinction between granitic dikes and leucosomes, suggesting a granite formation by in-situ anatexis. *[Langosch A. et al. , 2000]*. See My GeoGuide No. 24: The Uppermost Nappes of the Asterousia Mountains – from Apesokari to Lentas via Miamou.

In the Kali Limenes and Lendas areas, the igneous rocks are subordinate to metasedimentary amphibolite-facies rocks and the contact between both lithologies is not easily defined and mostly diffuse the field. The paragneisses forming the country rock have preserved ages of high-temperature metamorphism around 72 Ma. A granite from this area yields an identical age suggesting that magmatism and metamorphism occurred contemporaneously. *[Langosch A. et al. , 2000]*

Langosch A. et al, suggests that the Late Cretaceous plutonic rocks in the uppermost tectonic unit of Crete formed in a supra-subduction zone setting or, alternatively, during continental lithospheric extension from a depleted mantle. The granitoid compositions can be modelled by an assimilation-fractional crystallization process in which a diorite magma underwent fractional crystallization, accompanied by assimilation of (meta)sediments similar in composition to the amphibolite-facies metapelites in the area.

The intrusion of mafic melts at depth (not exposed in the ACC-mountains) might have acted as a heat source, elevating mid-crustal regions to amphibolite-facies temperatures and causing the formation of migmatite paragneisses. *[Langosch A. et al, 2000]*

2 Gerokampos to Agios Kyrillios

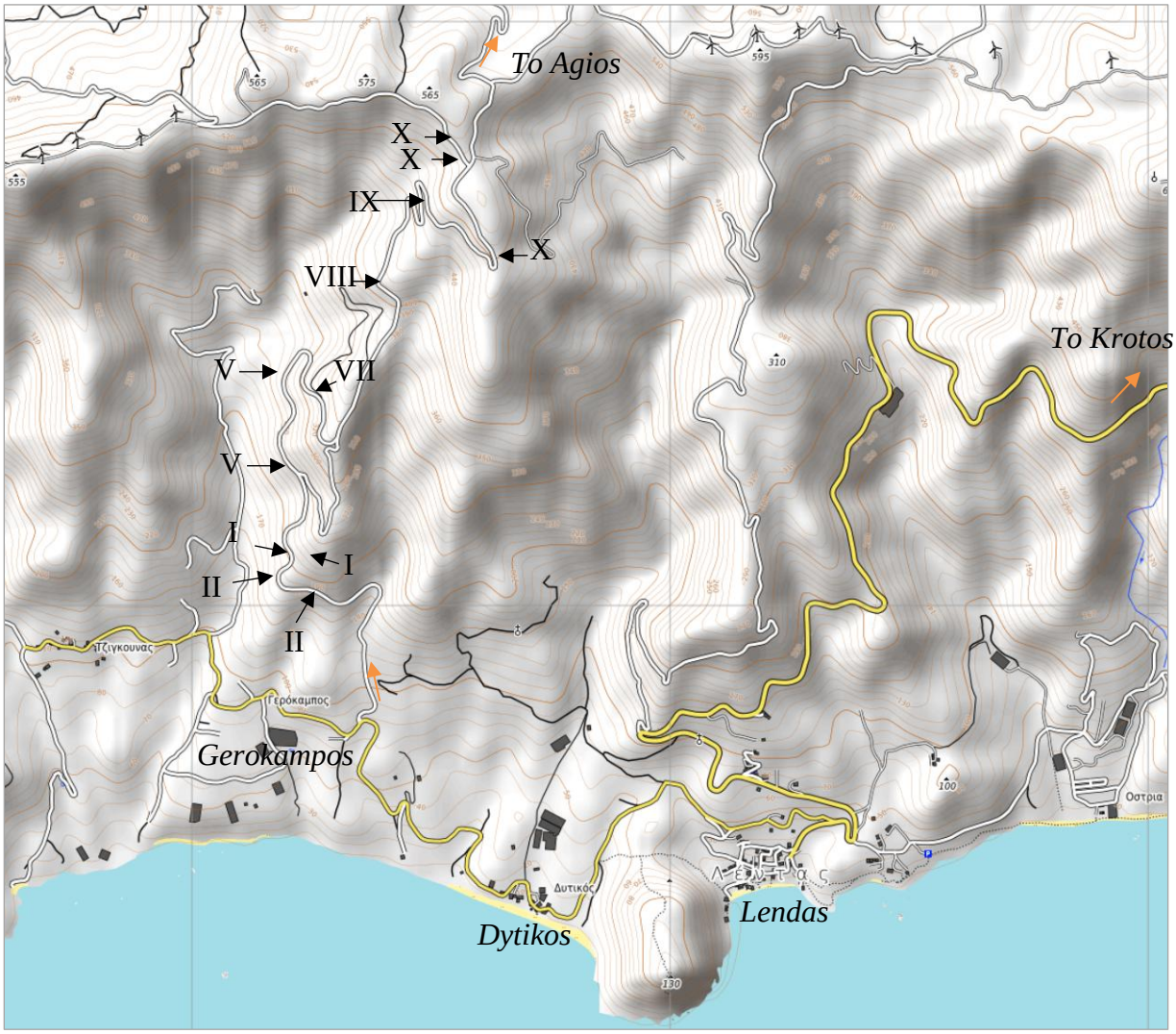

Location of outcrops along the road from Gerokampos to Agios Kyrillios

Location of outcrops I to VII [Source of image Google Maps]

Outcrop I. Calc-silicate schist.

Outcrop I. Calc-silicate schist.

Outcrop II. Paragneiss (metapelite). A paragneiss is a gneiss originating from sedimentary rock e.g a clay or silty sedimentary rock that has undergone HT/LP metamorphism of upper amphibolite facies.

Outcrop II Closeup of previous picture. The texture exhibits flow structures indicating the beginnings of anatexis (i.e. melting).

Outcrop II: a further example of early anatexis. 1: garnet crystal, 2: migmatite texture.

Outcrop III, view of the Lendas peninsular looking southeastwards from the road from Gerokampos to Agios Kirillios. The village of Dytikos is just visible at the coast.

Outcrop III. Highly weathered and jointed plutonic rock assumed to be of diorite composition owing to the lack of quartz. The outcrop displays numerous pegmatite veins and xenoliths. Xenoliths are inclusions of the country rock.

Outcrop III. Closeup of previous picture. Langosch A. et al. , 2000 indicates that the igneous rocks are related to the surrounding paragneisses and states that the difference between both lithologies is sometimes not easily seen in the field but appears more diffuse. The paragneiss forming the country rock has a preserved age of high-temperature metamorphism of around 72 Ma. The igneous rock from this area yields an identical age suggesting that magmatism and metamorphism occurred contemporaneously.

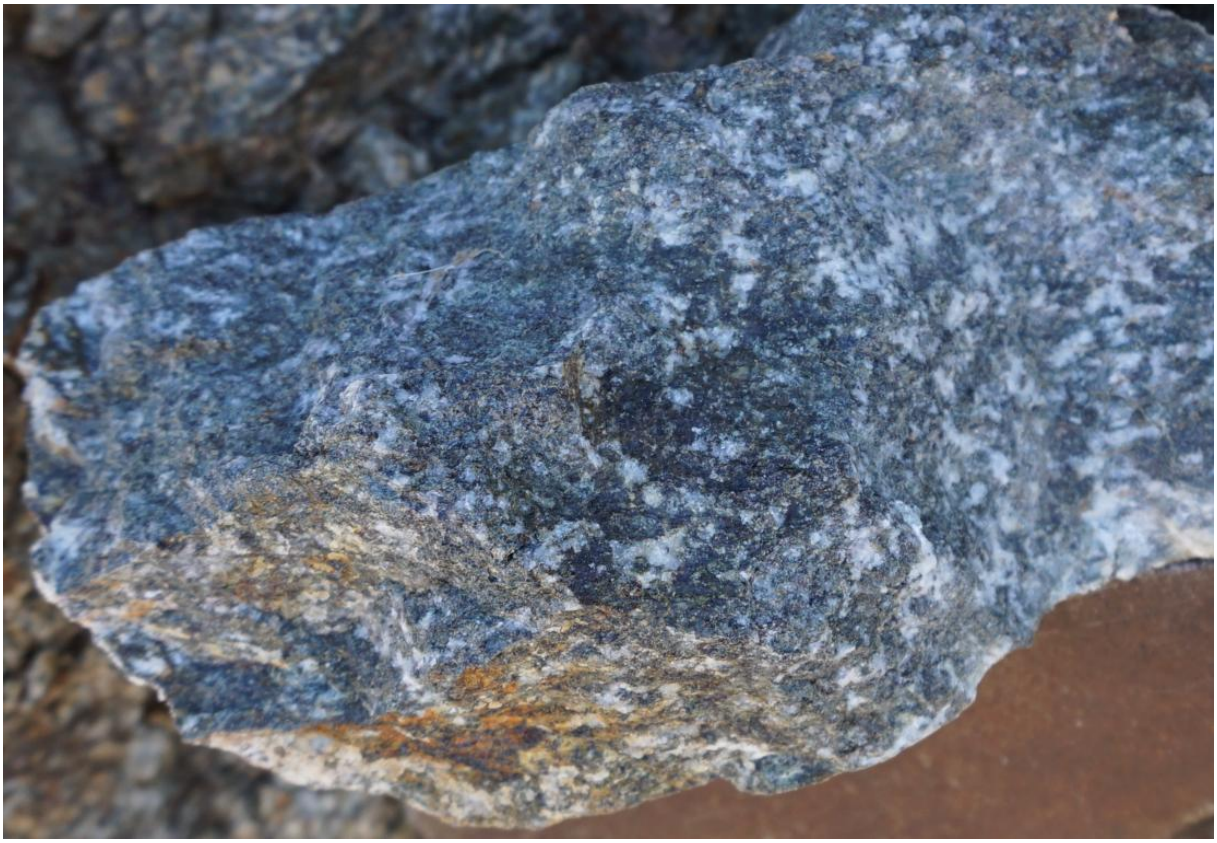

Outcrop III. Closeup of previous picture

Outcrop III. 1: Pegmatite vein cross cutting diorite rock. 1: dark border of vein indicates chemical interaction (i.e. metasomatism) with surrounding rock.

Outcrop III. Xenolith possibly consisting of former calc-silicate schist embedded in diorite. 1: overprinted calc-silicate schist, 2: diorite rock.

Outcrop III. Closeup of previous picture. 1: calc-silicate schist (now overprinted), 2: diorite rock, 3: chemical interaction at contact (i.e. metasomatism)

2.1 Assimilation-fractional crystallization (AFC)

AFC is an important process in igneous petrology whereby melts with widely differing isotopic and trace elements can be produced. When a primitive magma, such as a basalt, invades crustal rocks, portions of the country rock may become detached and be included in the magma as xenoliths. Because of the high temperature and thermal capacity of the basalt, it is capable of melting a proportion of the country rock. In doing so it loses some of its own heat and thus a proportion of the magma crystallizes. The composition of the resulting magma is determined by the relative amounts of magma and country rock initially present; the rates at which assimilation and crystallization proceed; and by the partition coefficients of the various elements between solid and liquid. *[Wikipedia]*

2.2 Diorites and quartz diorites

Diorites and quartz diorites of the Asterousia Mountains are found as coarse- and fine-grained varieties consisting of zoned plagioclase with An_{48} (core) to An_{30} (rim), clinopyroxene ($Wo_{45}En_{34}Fs_{21}$ with 0.7±2.4 wt % Al_2O_3), brown to green Ca-amphibole (tschermakite-magnesio/ferrohornblende), biotite and ilmenite. Some samples contain orthopyroxene ($Wo_2En_{46}Fs_{52}$) and/or clusters of cummingtonite/grunerite. Coarse-grained diorites with a high content of clinopyroxene have nearly undisturbed igneous textures, whereas Ca-amphibole-rich samples are clearly foliated. The fine-grained diorites always display a foliation caused by the alignment of pyroxene, plagioclase and biotite. In some cases fine-grained dioritic rocks are heterogeneous, showing compositional layering with changing proportions of clinopyroxene, Ca-amphibole, plagioclase, ilmenite and apatite. *[Langosch A. et al. , 2000]*

2.3 Rare Earth Elements (REE)

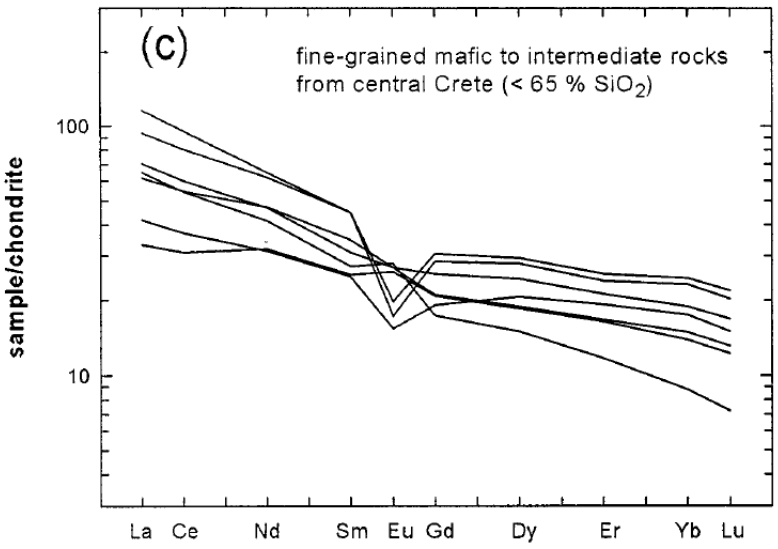

Normalized REE abundances in mafic to intermediate igneous rocks of the Astrousia Mts. Normalization is based on the chondrite values. Some of the rocks are characterized by a strong negative Eu anomaly indicating early fractionation of plagioclase and removal of Eu from the initial melt. [Langosch A. et al., 2000]

Outcrop III, 1: pegmatitic vein cross cutting both the paragneiss and diorite rock a few meters from the location described above. The pegmatite is not weathered and in a fresh condition. 2: paragneiss, 3: diorite. Based on the cross-cutting and fresh condition, the pegmatite vein was probably intruded at a later stage of events and is thought to be the leucosome of migmatite rocks found at other outcrops.

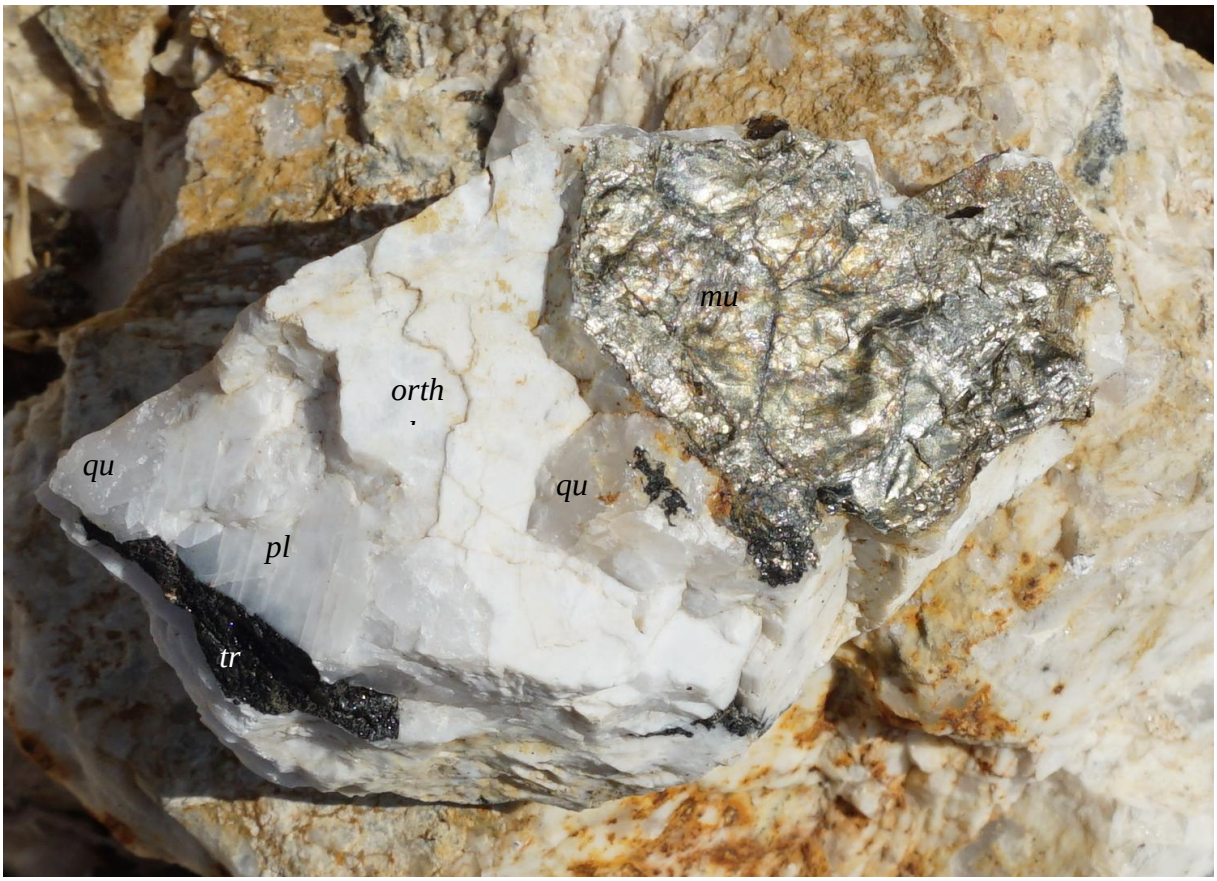

Outcrop III, sample from the pegmatitic vein. orth: orthoclase, pl: plagioclase, qu: quartz, mu: muscovite, tr: tourmaline?

Outcrop IV, Diorite displaying pegmatite texture and possible in-situ anatexis of paragneiss.

Outcrop IV: sample of weathered diorite rock. The rusty stains indicates oxidization of hornblende or other Fe-containing minerals.

Outcrop V, 1: paragneiss, 2: granitoid vein, 3: marble on top of the ridge

Outcrop V: View of the mountain side looking southeastwards. The country rock has numerous large and small normal faults indicating brittle "near" surface extensional deformation during a late stage of mountain building.

2.4 Leucosome

The leucosome is the lighter-coloured part of a migmatite, consisting predominantly of feldspar and quartz. The leucosome is derived from segregated partial melt and it may contain microstructures that indicate crystallisation from a melt or magma. The leucosome may not necessarily have the composition of an anatectic melt (i.e. in situ melting), as fractional crystallisation and separation of the fractionated melt may have occurred.

Leucosomes can be subdivided, depending on whether they are in situ, or they have segregated and migrated from their source (more on this below). In situ leucosomes may be distinguishable by the presence of a darker selvedge, comprising mafic minerals plus other minerals such as garnet or cordierite, which would represent the solid products of the melt reaction. In contrast, these features may be absent from injected leucosomes, where the melt has moved away from its source.

2.5 Leucosome Segrigation and Migration Features

The leucosome can be divided into several groups depending on the degree of separation from the site of melt production (Sawyer 2009). The distance travelled from the source can also affect the textural evolution of the leucosome, causing it to progress from something that is a minimum melt composition, to something that resembles a true granite. These groups also represent a progression in scale, from melt that is locally segregating at the grain-scale, up to large-scale magma, or melt, migration.

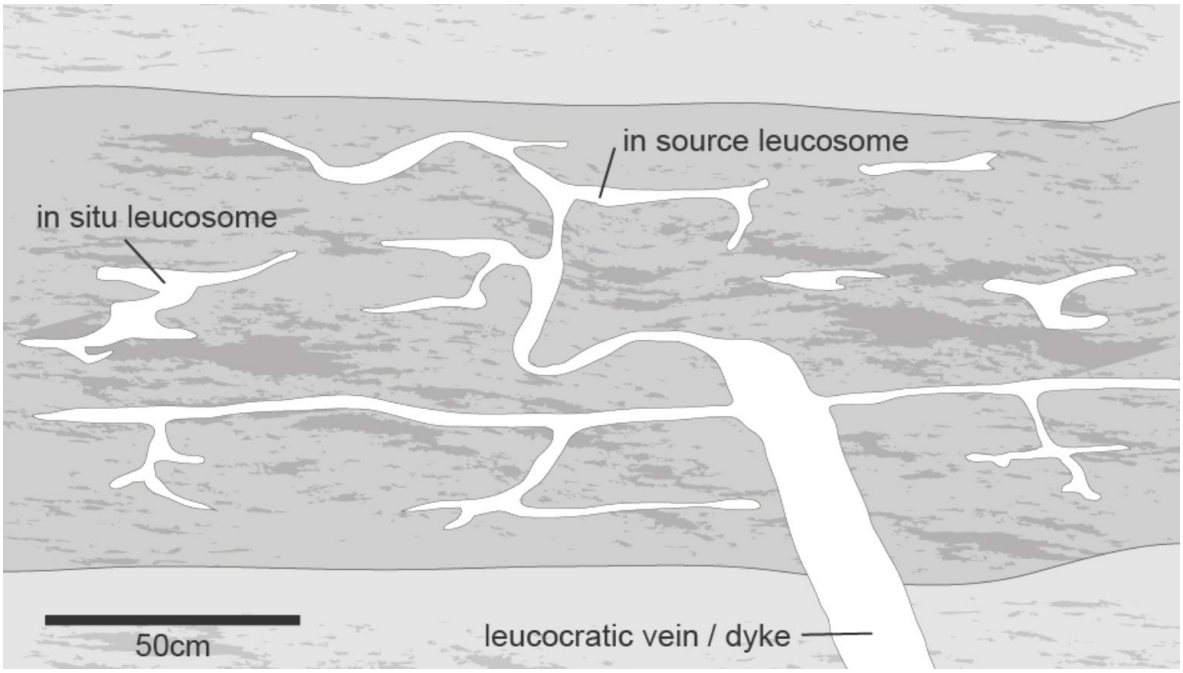

Schematic representation of a migmatite layer showing the difference between in situ, in-source and leucocratic vein or dykes (modified from Sawyer 2008b). [Pawley M. et. al., 2013]

In situ leucosome

This is the product of crystallisation of an anatectic melt, or part of a melt, that has segregated from the residuum but has remained at the site where the melt formed.

In-source leucosome

The product of crystallisation of an anatectic melt, or part of a melt, that has migrated away from the place where it formed but is still within the confines of its source layer.

Leucocratic vein or dyke

The product of crystallisation of an anatectic melt, or part of a melt, that has migrated out of its source layer and has been injected into another rock, which may be nearby or farther away, but is still in the region affected by the anatectic event. [Pawley M. et. al., 2013]

Outcrop V, 1: Paragneiss, 2: Granitoid vein. Fragments of country rock embedded within the vein indicate brittle deformation of the country rock during intrusion of pegmatitic fluids. The vein consists of feldspar and some quartz but has no mafic minerals and is probably an "in-source leucosome.

Outcrop V. Sample of paragneiss/ calc-silicate schist. Foliation is parallel to bedding. 1: the light brown and grey-green layers are calcareous.

Outcrop VI. One of two marble bodies located on this mountain side. 1: Marble body within metapelite displaying clean distinct boundaries. The irregular contact to the metapelite is due to offsetting by numerous normal faults creating a type of "graben and horst" structure. 2: Weathered metapelite.

Outcrop VI. Dark lines within the marble mark bedding planes.

Outcrop VI. The marble is coarse grained owing to HT/LP (high temperature / low pressure) metamorphism and is likely to have been exposed to the same tectonic and metamorphic conditions as the metapelite. The scratch marks are from a hardened steel nail.

Outcrop VI. Normal faults have offset the marble and metapelite, indicating brittle deformation at a later post-metamorphic period.

Outcrop VI. 1: Metapelite underlying the marble body. 1: Former bedding planes, 2: Hand sample (see next picture)

Outcrop VI. Closeup of previous picture. Sample from the metapelite displaying foliation (i.e. alinement of minerals perpendicular to direction of stress. Minerals are thought to be predominantly light and dark mica as well as feldspar (macroscopic assessment).

Outcrop VI. Overview of the outcrop from a different angle showing multiple normal faults.

Outcrop VI. 1: Former bedding within the metapelite cut by a fault. 2: Numerous thin veins indicate joints and fissures filled with secondary minerals

Outcrop VII. Overview of the upper marble body.

Outcrop VII. The irregular shape of the contact to the marble body is due to post-metamorphic faulting. 1: Metapelite displaying former bedding planes and foliation parallel to bedding, 2: Fractured marble

Outcrop VII. Metapelite displaying former bedding planes

Outcrop VII. Closeup of previous picture. The metapelite is foliated parallel to former bedding and displays predominantly light and dark mica as well as feldspar (macroscopic assessment).

Outcrop VII. Contact between metapelite and marble body. At this spot there appears to have been a former alternating deposition of limestone and clay/silt. The contact is sedimentary and not magmatic. 1: former thin limestone bed, 2: former clay/silt layer, 3: marble body. 4: fault

Location of Outcrops VIII to XII [Source of image Google Maps]

Outcrop VIII. View of the valley and coast from the ophiolite body. Ultramafic rock in the foreground.

Outcrop VIII. Overview of the ultramafic body. Rucksack as scale

Outcrop VIII. Ultramafic rock containing pyroxene phenocrysts. 1: pyroxene

Outcrop VIII. White serpentinite originating from the ultramafic rock.

Outcrop VIII. Highly sheared gneiss lenses bordering the ultramafic body indicating emplacement of the ultramafic body by shear tectonics.

Outcrop IX. Calc-silicate schist / marble

Outcrop IX. Calc-silicate schist / marble

Outcrop X. Shear zone displaying lens shaped forms and possible formation of skarn. The blue vein indicates an interaction of carbonate containing rock with hydrothermal fluids.

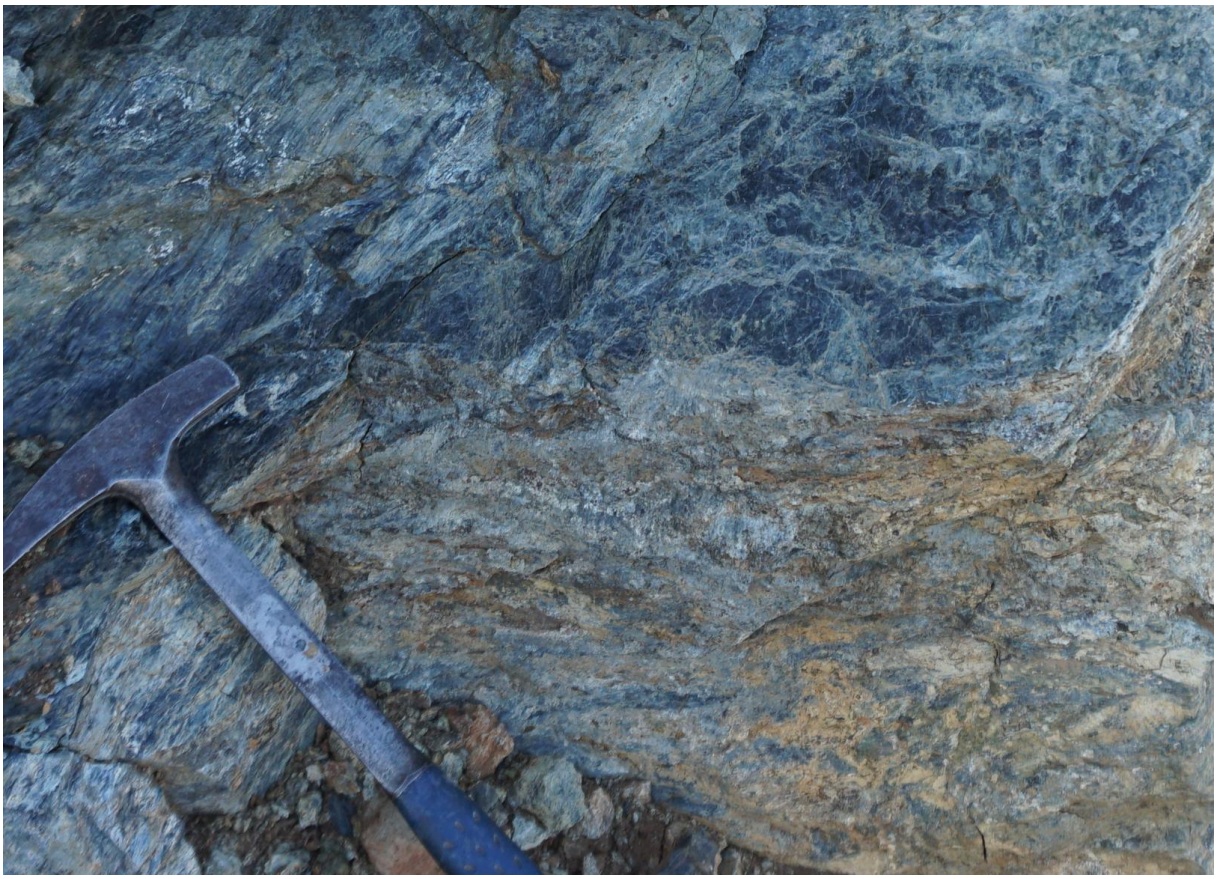

Outcrop X. Close up of previous picture. The dark blueish vein appears to be the fault along which hydrothermal fluids have travelled.

Outcrop X. Lens-shaped body that could be a skarn.

Outcrop X. Closeup of a sample from the lens-shaped body.

2.6 Skarn

Skarn is a type of hard, coarse-grained metamorphic rock that forms through the hydrothermal alteration of pre-existing rocks, typically carbonate-rich rocks like limestone or dolomite. Skarns are often associated with contact metamorphism where hot fluids from intruding magma alter the surrounding rock, resulting in the formation of distinct mineral assemblages and textures characteristic of skarns. These rocks can contain a variety of minerals such as garnet, pyroxene, and calc-silicates depending on the composition of the original rock and the nature of the hydrothermal fluids involved in their formation. https://www.wikiwand.com/en/Skarn

Outcrop XI. Quartz vein in Amphibolite. 1: Amphibolite, 2: Quarz

Outcrop XI. Amphibolite

Outcrop XI. Close up of previous picture showing amphibolite sample

Outcrop XI. Quartz from quartz vein. Notice the trail of steel left from scratching the surface with a nail.

Outcrop XII. Marble body in cataclastic amphibolite. Cataclastites are created in brittle fault zones and are often found within shear zones of nappes. 1: Marble, 2: cataclastite.

Outcrop XII. Cataclastic texture of the amphibolite bordering the marble lens

Outcrop XII. Closeup of previous picture

Outcrop XII. Sample from the marble lens. The surface is easily scratched with a steel nail

View of the Messara basin after traversing the Asterousia Mts. looking North. In the background the Psilorities Mts consisting predominantly of Plattenkalk limestone. The Psilorities foothills are of Neogene age and are primarily composed of yellowy limestone, sand and silt beds with occasional gypsum deposits.

References

Alexandra van der Geer1 & George Lyras, 2011: Field Trip Guidebook European Association of Vertebrate Palaeontologists, 9th Annual Meeting Heraklion, Crete, Greece 14-19 June, 2011

Alves, T. Cupkovic T., 2018: Footwall degradation styles and associated sedimentary facies distribution in SE Crete: Insights into tilt-block extensional basins on continental margins; 3D Seismic Lab, School of Earth and Ocean Sciences, Cardiff University, Cardiff, United Kingdom; Husky Energy, Atlantic Region, 351 Water St., Suite 105, St. John's, Canada

Brack P., Meister P. H., Bernasconi S., 2013: Dolomite formation in the shallow seas of the Alpine Triassic, Article in Sedimentology · Feb. 2013, DOI: 10.1111/sed.12001]

Brandes C. et al., 2014: Fault-related folding: A review of kinematic models and their application, Institute for Geology, Leibniz Universität Hannover, Callinstr. 30, 30167 Hannover, Germany

Champod E. et al., 2010: Stampfli Field Course: Tectonostratigraphy and Plate Tectonics of Crete, Université de Lausanne, September 2010

Chatzaras, v., Xypolias, P. & Doutsos, T (2006): Exhumation of high-pressure rocks under continuous compression: a working hypothesis for the southern Hellenides (central Crete. Greece). - Geol. Mag. 143: 859-R76.

Cowan (1985), Gesteine bestimmen, Teil 2: Minerale
https://www.kristallin.de/gesteine/index.htm

Fassoulas C., 2000: The tectonic development of a Neogene basin at the leading edge of the active European margin: the Heraklion basin, Crete, Greece, Natural History Museum of Crete, University of Crete, Heraklion 71409, Greece

Fassoulas C., Rahl J.M., 2004: Patterns and Conditions of Deformation in the Plattenkalk Nappe, Crete, Greece: A Preliminary Study, Natural History Museum of Crete, Yale University, New Haven, Connecticut

Granger D.E., 2007: Cosmogenic Nuclide Dating - Landscape Evolution, in Encyclopedia of Quaternary Science, Pages 445-452

Koepke J. et. al., 2004: Hornblendites within Ophiolites of Crete, Grecce: Evidence for Amphilole-rich Cumulates derived from an iron-rich Tholeiitic Melt, Institut für Mineralogie, Universität Hannover, Germany

Kull U., 2012: Kreta, Sammlung geologischer Führer

Lacinska A. M. et. al., 2016: Mineralogical characterisation of serpentine minerals in the context of carbon capture and storage by mineralization. Preliminary results, British Geological Survey, Environmental Science Centre, Nicker Hill, Keyworth, Nottingham NG12 5GG, United Kingdom

Langosch A. et al, 2000: Intrusive rocks in the ophiolitic melange of Crete ± Witnesses to a

Late Cretaceous thermal event of enigmatic geological position, Institut für Mineralogie und Geochemie, Universität zu Köln.

Martha S. et. al., 2018: The tectonometamorphic evolution of the Uppermost Unit south of the Dikti Mountains, Crete

McClay K.R.: Glossary of thrust tectonics terms, Department of Geology, Royal Holloway and Bedford New College, University of London, Egham, Surrey, England

Miller W., 1977: Geologie des Gebites Nördlich des Plakias-Bucht, Kreta, Freiburg im Breisgau, Diplomarbeit

Mountrakis D., Kilias A., Pavlaki A., Fassoulas C., Thomaidou E., Papazachos C., Papaioannou C., Roumelioti Z., et al., 2012: Neotectonic study of Western Crete and implications for seismic hazard assessment, Journal of the Virtual Explorer, Electronic Edition, ISSN 1441-8142, volume 42, paper 2 In: (Eds.) Emmanuel Skourtsos and Gordon S. Lister, The Geology of Greece, 2012.

Ogata K. et. al., 2013: Mélanges in flysch-type formations: Reviewing geological constraints for a better understanding of complex formations with block-in-matrix fabric, Universita` degli Studi di Napoli Federico II, Dipartimento di Scienze della Terra

Palamakumbura R. et. al., 2012: Geochemical, sedimentary and micropaleontological evidence for a Late Maastrichtian oceanic seamount within the Pindos ocean (Arvi Unit, S Crete, Greece), School of GeoSciences, University of Edinburgh, West Mains Road, Edinburgh, EH9 3JW, UK

Pawley M. et. al. 2013: A user's guide to migmatites, Geological Survey of South Australia, Resources and Energy Group, DMITRE Report Book 2013/00016

Pirazzoli P.A., Thommeret J., Thommeret Y., Laborel J., and Montaggioni L.F., 1982: Tectonophysics 86, 27-43.

Pomoni F., Karakitsios V., 2016: Sedimentary facies analysis of a high-frequency, small-scale, peritidal carbonate sequence in the Lower Jurassic of the Tripolis carbonate unit (central western Crete, Greece): Long-lasting emergence and fossil laminar dolocretes horizons, Department of Geology and Geoenvironment, National and Kapodistrian University of Athens

Rahl J. M. et. al.: Exhumation of high-pressure metamorphic rocks within an active convergent margin, Crete, Greece: A field guide, Jeffrey M. Rahl, Charalampos, Fassoulas, and Mark T. Brandon, Department of Geology and Geophysics, Yale University, New Haven, Connecticut 06511, U.S.A. Natural History Museum of Crete, University of Crete, Heraklion 71409, Greece

Rieger S., 2015: Regional-Scale, Natural Persistent Scatterer Interferometry, Island of Crete (Greece), and Comparison to Vertical Surface Deformation on the Millennial-, and Million-Year Time-Scales; Phd.; Ludwig-Maximilians-Universität München

Seidel M., 2003: Tectono-sedimentary evolution of middle Miocene supra-detachment basins (western Crete, Greece), Ph.D. Dissertation, University of Köln.

Stampfli 2010: Stampfli Field Course, Tectonostratigraphy and Plate Tectonics of Crete, Université de Lausanne, France

Steiakakis E., 2017: Evaluation of Exploitable Groundwater Reserves in Karst Terrain: A Case Study from Crete; Greece Laboratory of Applied Geology, Technical University of Crete, 73100 Chania, Greece

Thomson S. N. et al., 1998: Apatite fission-track thermochronology of the uppermost tectonic unit of Crete, Implications for the post-Eocene tectonic evolution of the Hellenic Subduction System, Institut für Geologie, Ruhr-Universität Bochum

Thomson S. N., Stockert B., Brix M. R., 1999. Miocene high-pressure metamorphic rocks of Crete, Greece: rapid exhumation by buoyant escape. In: Ring, U., Brandon M. T., Lister G. S., Willetf S. D. (eds): Exhumation Processes: Normal Faulting, Ductile Flow and Erosion. Geological Society, London, Special Publications, 154, 87-107.

Thomson S. N., Stockhert, B. & Brix, M.R. (1998a): Thennochronology of the high-pressure metamorphic rocks of Crete, Greece: implications for the speed of tectonic processes. - Geology 26: 259-262.

Thrust faults: Some common terminology - Geological Digressions https://www.geological-digressions.com

Tiberti M. M., Basili R. & Vannoli P., 2014: Ups and downs in western Crete (Hellenic subduction zone), Istituto Nazionale di Geofisica e Vulcanologia, Via di Vigna Murata 605, 00143 Rome, Italy

Theye, T, Seidel, E. & Vidal, O. (1992): Carpholite, sudoite and chloritoid in low-grade high-pressure metapelites from Crete and the Peloponnese, Greece. - Europ, J. Mineral.4 487-507.

Tortorici L., 2011: The Cretan ophiolite-bearing mélange (Greece): A remnant of Alpine accretionary wedge, Dipartimento di Scienze Geologiche, University of Catania, C.so Italia 55, 95129 Catania, Italy

van Hinsbergen D. J. J., Meulenkamp J. E., 2006: Neogene supradetachment basin development on Crete (Greece) during exhumation of the South Aegean core complex.

Vassilakis E. and Alexopoulos J., 2012: Recognition of Strike-slip Faulting on the Supradetachment Basin of Messara (Central Crete) with remote sensensing Image Interpretation Techniques; National and Kapodistrian University, Department of Dynamics, Tectonics and Applied Geology, Athens, Greece; National and Kapodistrian University, Department of Geophysics & Geothermics, Athens, Greece;

Wassmann S., 2012 Geländekurs Kreta

Zachariasse W., van Hinsbergen D., et al. 2011, Formation and Fragmentation of a late Miocene supradetachment basin in central Crete: implications for exhumation mechanisms of high-pressure rocks in the Aegean forearc, Stratigraphy and Paleontology group, Faculty of Geosciences, Utrecht University, Utrecht, The Netherlands; Physics of Geological Processes, University of Oslo

Appendix

Geological Time Scale

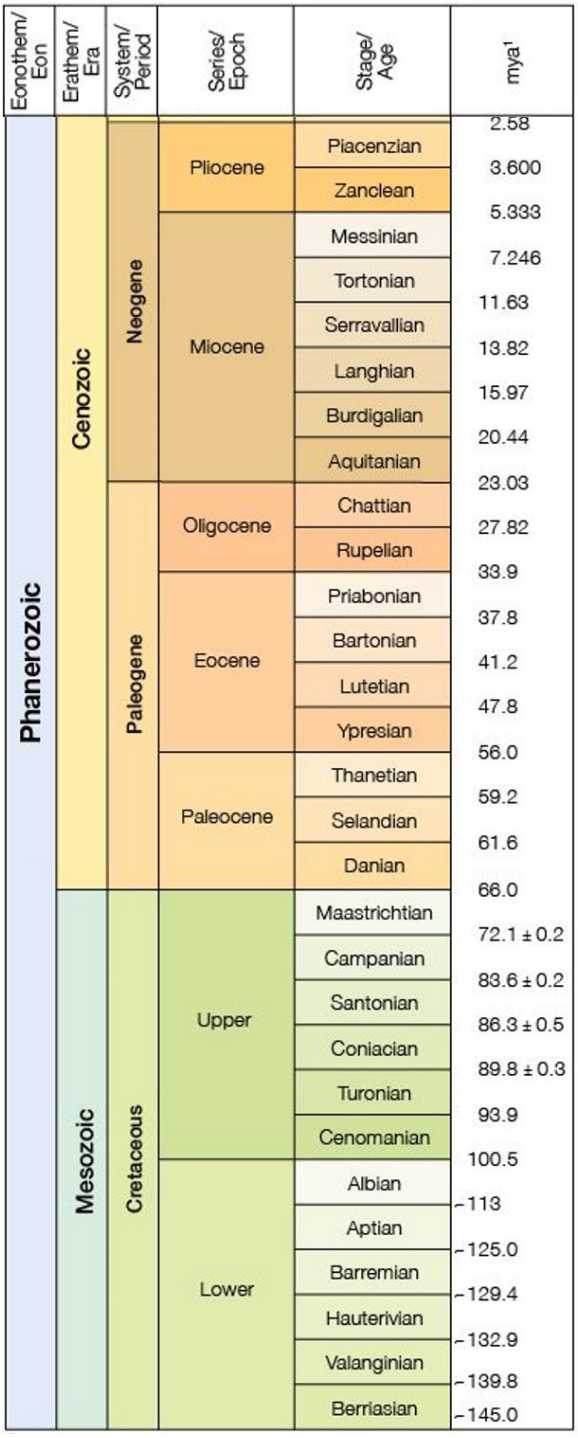

Eonothem/ Eon	Erathem/ Era	System/ Period	Series/ Epoch	Stage/ Age	mya[1]
Phanerozoic	Cenozoic	Neogene	Pliocene	Piacenzian	2.58
				Zanclean	3.600
			Miocene	Messinian	5.333
				Tortonian	7.246
				Serravallian	11.63
				Langhian	13.82
				Burdigalian	15.97
				Aquitanian	20.44
		Paleogene	Oligocene	Chattian	23.03
				Rupelian	27.82
			Eocene	Priabonian	33.9
				Bartonian	37.8
				Lutetian	41.2
				Ypresian	47.8
			Paleocene	Thanetian	56.0
				Selandian	59.2
				Danian	61.6
	Mesozoic	Cretaceous	Upper	Maastrichtian	66.0
				Campanian	72.1 ± 0.2
				Santonian	83.6 ± 0.2
				Coniacian	86.3 ± 0.5
				Turonian	89.8 ± 0.3
				Cenomanian	93.9
			Lower	Albian	100.5
				Aptian	~113
				Barremian	~125.0
				Hauterivian	~129.4
				Valanginian	~132.9
				Berriasian	~139.8
					~145.0

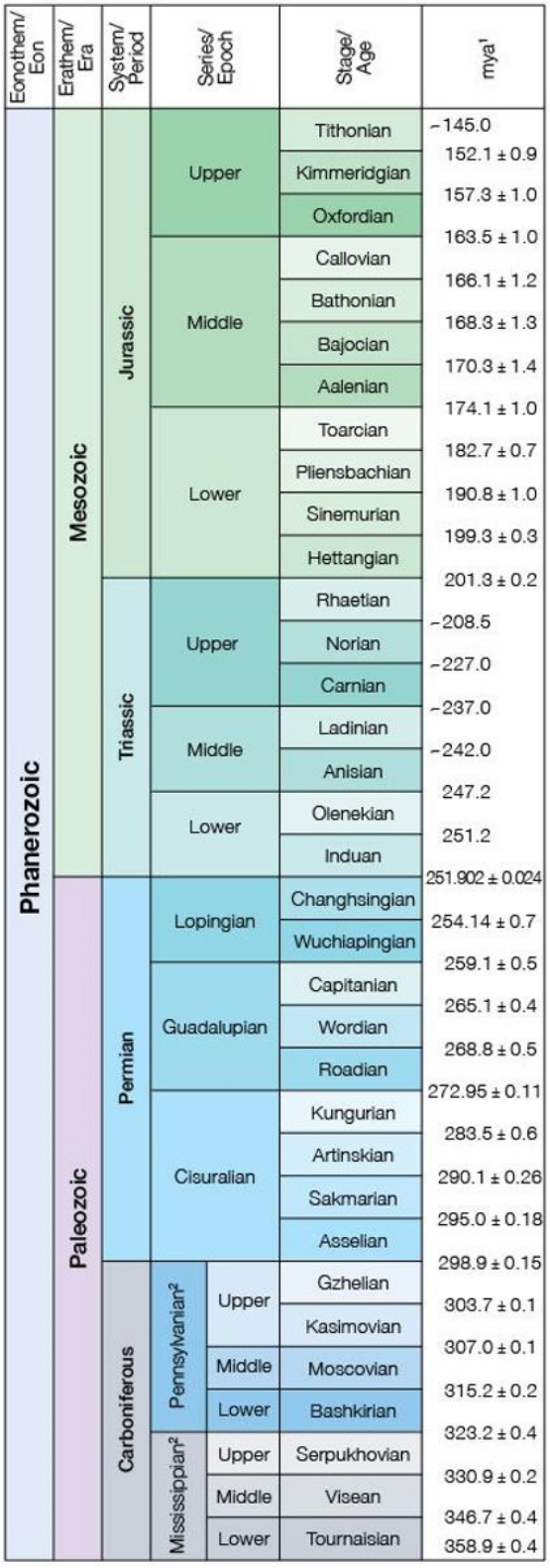

Eonothem/ Eon	Erathem/ Era	System/ Period	Series/ Epoch		Stage/ Age	mya[1]
Phanerozoic	Mesozoic	Jurassic	Upper		Tithonian	~145.0
					Kimmeridgian	152.1 ± 0.9
					Oxfordian	157.3 ± 1.0
			Middle		Callovian	163.5 ± 1.0
					Bathonian	166.1 ± 1.2
					Bajocian	168.3 ± 1.3
					Aalenian	170.3 ± 1.4
			Lower		Toarcian	174.1 ± 1.0
					Pliensbachian	182.7 ± 0.7
					Sinemurian	190.8 ± 1.0
					Hettangian	199.3 ± 0.3
		Triassic	Upper		Rhaetian	201.3 ± 0.2
					Norian	~208.5
					Carnian	~227.0
			Middle		Ladinian	~237.0
					Anisian	~242.0
			Lower		Olenekian	247.2
					Induan	251.2
	Paleozoic	Permian	Lopingian		Changhsingian	251.902 ± 0.024
					Wuchiapingian	254.14 ± 0.7
			Guadalupian		Capitanian	259.1 ± 0.5
					Wordian	265.1 ± 0.4
					Roadian	268.8 ± 0.5
			Cisuralian		Kungurian	272.95 ± 0.11
					Artinskian	283.5 ± 0.6
					Sakmarian	290.1 ± 0.26
					Asselian	295.0 ± 0.18
		Carboniferous	Pennsylvanian[2]	Upper	Gzhelian	298.9 ± 0.15
					Kasimovian	303.7 ± 0.1
				Middle	Moscovian	307.0 ± 0.1
				Lower	Bashkirian	315.2 ± 0.2
			Mississippian[2]	Upper	Serpukhovian	323.2 ± 0.4
				Middle	Visean	330.9 ± 0.2
				Lower	Tournaisian	346.7 ± 0.4
						358.9 ± 0.4

Metamorphic evolution of the Asterousia Crystalline Complex (ACC) by Martha S. et. al.

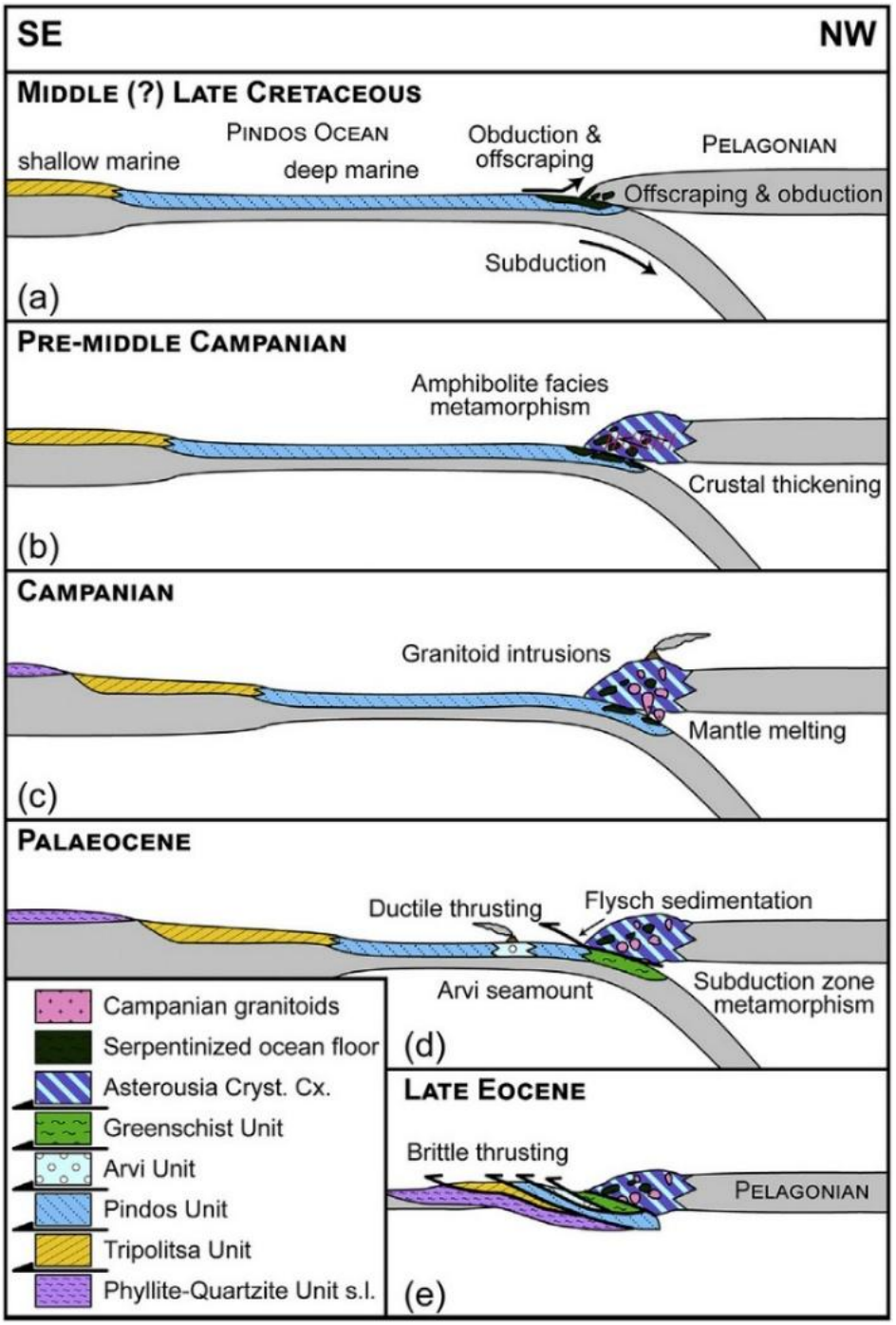

Model depicting the sequences of tectonic events within the Asterousian Mountains [Martha S. and Zulauf G. et. al., 2018].

Work by Martha S. and Zulauf G. et. al., 2018 south of the Dikti mountains indicates that the ACC-type rocks have been affected by polyphase deformation (D1–D3) and metamorphism. Relics of the D1 phase are preserved as internal foliation in garnet porphyroblasts. D2 top-to-the SE shearing under upper amphibolite facies conditions led to the dominant foliation. After post-D2 exhumation, parts of the ACC-type rocks south of the Dikti Mts. were affected by contact metamorphism of a non-exposed pluton, which intruded at a depth below 10 km during Campanian time (74±2Ma; mass spectrometry on zircon). This age, is in line with intrusion ages of ACC-type (meta)granitoids exposed on Crete. The S2-foliation of the ACC-type rocks was reactivated during the late phase of contact metamorphism by D3 top-to-the SE shearing. During middle Paleocene time, the ACC nappe was thrust on top of the other Uppermost units. This thrusting event as well as subsequent brittle thrusting of the ACC-type rocks on top of the prehnite-pumpellyite facies metamorphic Arvi Unit was still accommodated by top-to-the SE kinematics, which is the dominant kinematics of the Uppermost Unit on Crete.

Apatite Fusion Track Ages - Metamorphic Cooling by Thomson S. N., 1998

Introduction

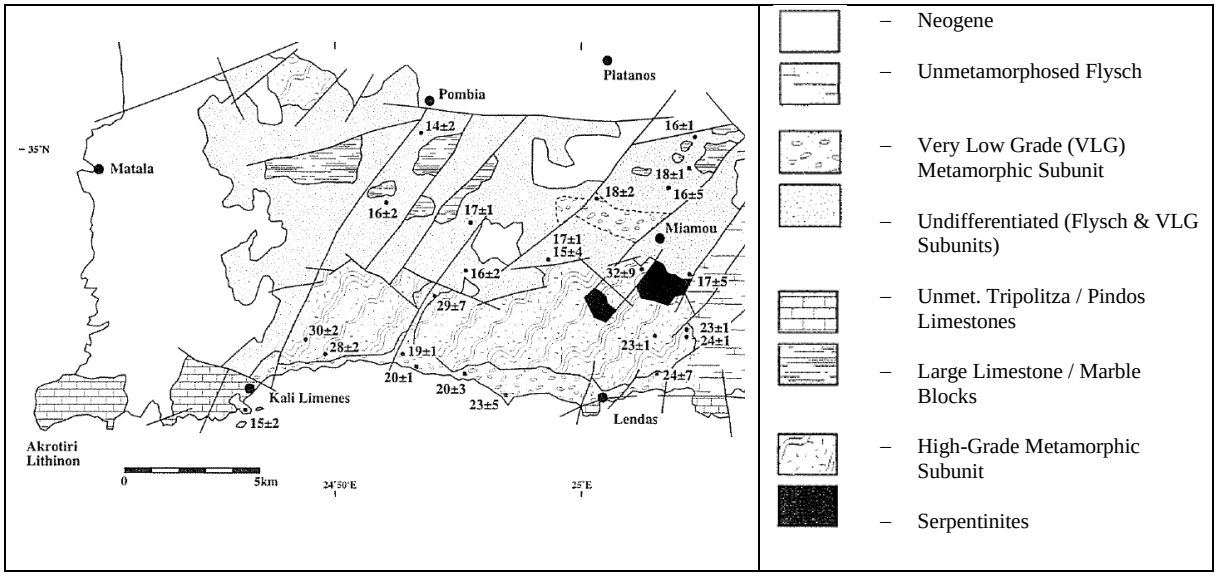

Figure 4. Simplified geological and location map showing the apatite fission-track central ages obtained from the various components of the uppermost tectonic unit exposed in the region of Lendas, southern Crete. [Thomson S. N., 1998]

The uppermost tectonic unit (UM Unit) of the Cretan nappe pile comprises a number of differing components. Three of the sub-units existing at the Asterousia Mts. are discussed here. The uppermost nappes overlie Pindos limestone and Pindos Flysch. The flysch sequence is of Lower to Middle Eocene (Aubouin et al., 1965) age and consists of sandstones, shales and calc-turbidites and has flysch-like character. These pass downward into a typical Pindos facies of basinal (deep marine) sedimentary rocks of Late Triassic to Palaeocene age that include pelagic limestones, radiolarites, calc-turbidites and calcbreccias (Seidel, 1971). In places the sequence passes up into a 'Blocky Flysch' that contains large (100's meter scale) shelf limestone blocks of Mesozoic to Eocene age as well as abundant clasts of granite, metamorphic rocks and serpentinite (Bonneau, 1984).

The Very Low Grade Metamorphic Subunit (VLG)

This subunit, parts of which have been described as the 'Arvi Nappe' (Bonneau, 1972), includes pillow-basalts, tuffs, dolerite dykes, turbiditic psammites and sedimentary 'mass-flows' and red pelagic limestones of Late Cretaceous age. Petrologic studies (Robert & Bonneau, 1982; Hall, 1987) show these rocks have been altered at low temperatures, with formation of pumpellyite, epidote, chlorite, calcite and muscovite, commonly in amygdales and veins. This has been considered to represent sub-sea floor metamorphism due to hydrothermal circulation (Bonneau, 1984). This subunit tectonically overlies, but is always found in close association with the Pindos Unit.

The High Grade Metamorphic Subunit (HGM)

This subunit, often referred to as the 'Asterousia Nappe' (Bonneau, 1972), consists of high-grade metamorphic rocks that include amphibolite, marbles, mica schists, migmatites and leucogranites (Creutzburg & Seidel, 1975). Seidel et al. (1976; 1981) have demonstrated high temperature-low pressure conditions of metamorphism and K-Ar ages from hornblende and biotite of ca. 70-75Ma (Late Cretaceous).

The Ophiolite Subunit

The highest rocks of the Cretan nappe pile comprise mainly serpentinite with, in places, associated basic dykes and Jurassic-Cretaceous sedimentary rocks. These are found as relict nappes thrust upon the rocks of the HGM Subunit. K-Ar age determinations yield ages of 140 to 156 Ma (Seidel et al., 1981). These authors also propose that these rocks were formed as ophiolites in either an island arc or continental margin environment.

Apatite Fusion Track Ages

In the Lendas area the apatite Fusion Track (FT) ages are relatively wide spread from 14.0±1.7 Ma to 32.0±8.8 Ma. The data from the flysch rocks give apatite FT ages of between 14.0±1.7 Ma and 17.7±1.0 Ma. Interpretation of these results indicates that the flysch cooled quickly through the apatite partial annealing zone between ca. 19 and 13 Ma. The apatite FT ages from the VLG rocks of the Lendas area are generally slightly older, being between 15.1±2.1 Ma and 20.0 ±5Ma. The HGM Subunit rocks of the UGM Unit give significantly older apatite FT ages than the VLG rocks, ranging from 20.0±2.5 Ma to 30.8±2.5 Ma.

Thermal History Modelling

The Flysch Unit rocks must have been at the surface (i.e., 20°C) when they were unconformably overlain by the onset of Neogene sedimentation between ca. 15 Ma and 12 Ma (Postma et al., 1993). The majority of the unmetamorphosed flysch was deposited during the Eocene, thus these samples are constrained by their depositional age. However, as these rock samples have been totally annealed during the Miocene, the older 'burial' or heating of these samples cannot be predicted by thermal history modelling. The depositional age is included in the following figure only to illustrate that these rocks must have been significantly buried after deposition. The VLG metamorphic rocks of probable late Mesozoic age (Seidel et al., 1977), were probably not buried during the late Eocene / early Oligocene. Hence for these samples the T-t history starts from below the apatite annealing zone. The thermal history of the HGM rocks is constrained by radioisotope dating of hornblende, muscovite and biotite, which indicates K-Ar ages of ca. 70 Ma (Seidel et al., 1981). This indicates rapid late Cretaceous cooling to below the closure temperature of Ar in biotite (ca. 320°C – Harrison et al., 1985).

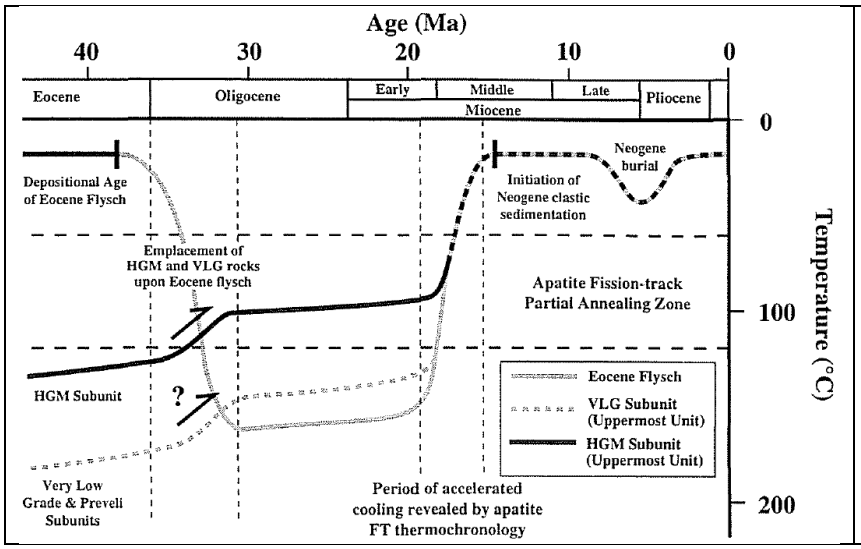

Figure 8. Proposed late Tertiary cooling history of the components of the uppermost tectonic unit in the area around Lendas, southern Crete deduced from apatite fission-track thermochronology and other structural and stratigraphic constraints [Thomson S. N., 1998]

Conclusions

The rocks of the Pindos, Tripoliza and Upper Most nappes are thought to have undergone a period of extension and accelerated erosion during the Middle Miocene (ca. 17 Ma). Today's exposure of the base of the apatite partial annealing zone at the earth's surface enables a good estimation of the total thickness of rock that was eroded away during that time. The erosion of approx. 4km rock implies a mean denudation rate of ca. 650m/m.y.

In addition, the presence of older apatite FT ages with corresponding bi-modal track length distributions from the high-grade metamorphic rocks of the upper Most tectonic unit, require that no significant denudation occurred at the surface during the accretion of the Cretan tectonic units, including the burial to ca. 35km and subsequent denudation of the HP/LT Phyllite-Quartzite and Plattenkalk Units, between the Oligocene and Early Miocene.

Given this information Thomson S. N. (1998) proposes a tectonic model for the evolution of the Cretan segment of the Hellenic Subduction Zone that requires a continuously retreating subduction zone boundary since at least the Late Eocene. The subsequent onset of accelerated erosion during the Middle Miocene is attributed to a change in the plate tectonic regime associated with the accretion of the Adria continental microplate and its sedimentary deposits of the Pindos, Tripolitza and lower HP-LT Units (Plattenkalk and Quartzite-Phyllite Units).

Fission track dating

A radiometric dating technique

Fission track dating is a radiometric dating technique based on analyses of the damage trails, or tracks, left by fission fragments in certain uranium-bearing minerals and glasses. Fission-track dating is a relatively simple method of radiometric dating that has made a significant impact on understanding the thermal history of continental crust, the timing of volcanic events, and the source and age of different archaeological artifacts. The method involves using the number of fission events produced from the spontaneous decay of uranium-238 in common accessory minerals to date the time of rock cooling below closure temperature. Fission tracks are sensitive to heat, and therefore the technique is useful at unraveling the thermal evolution of rocks and minerals. Most current research using fission tracks is aimed at: a) understanding the evolution of mountain belts; b) determining the source or provenance of sediments; c) studying the thermal evolution of basins; d) determining the age of poorly dated strata; and e) dating and provenance determination of archeological artifacts.

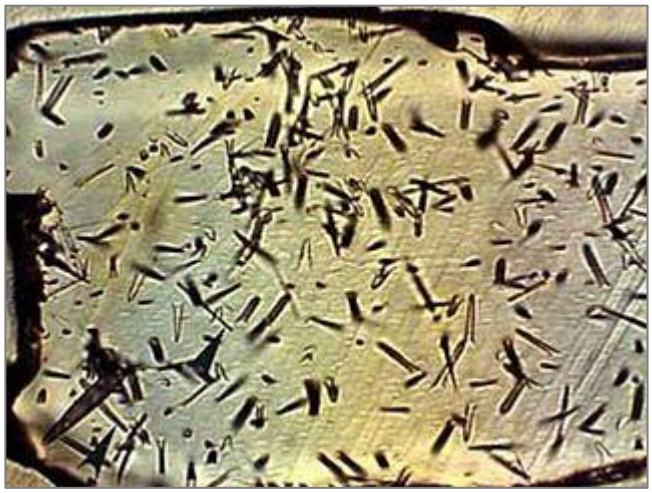

Etched fission tracks from 238 uranium in apatite. track lengths are approximately 17 microns.

In the 1930s it was discovered that uranium (specifically U-235) would undergo fission when struck by neutrons. This caused damage tracks in solids which could be revealed by chemical etching.

Method

Unlike other isotopic dating methods, the "daughter" in fission track dating is an effect in the crystal rather than a daughter isotope. Uranium-238 undergoes spontaneous fission decay at a known rate, and it is the only isotope with a decay rate that is relevant to the significant production of natural fission tracks; other isotopes have fission decay rates too slow to be of consequence. The fragments emitted by this fission process leave trails of damage (fossil tracks or ion tracks) in the crystal structure of the mineral that contains the uranium. The process of track production is essentially the same by which swift heavy ions produce ion tracks. Chemical etching of polished internal surfaces of these minerals reveals spontaneous fission tracks, and the track density can be determined. Because etched tracks are relatively large (in the range 1 to 15 micrometres), counting can be done by optical microscopy, although other imaging

techniques are used. The density of fossil tracks correlates with the cooling age of the sample and with uranium content, which needs to be determined independently.

To determine the uranium content, several methods have been used. One method is by neutron irradiation, where the sample is irradiated with thermal neutrons in a nuclear reactor, with an external detector, such as mica, affixed to the grain surface. The neutron irradiation induces fission of uranium-235 in the sample, and the resulting induced tracks are used to determine the uranium content of the sample because the 235U:238U ratio is well known and assumed constant in nature. However, it is not always constant. To determine the number of induced fission events that occurred during neutron irradiation an external detector is attached to the sample and both sample and detector are simultaneously irradiated by thermal neutrons. The external detector is typically a low-uranium mica flake, but plastics such as CR-39 have also been used. The resulting induced fission of the uranium-235 in the sample creates induced tracks in the overlying external detector, which are later revealed by chemical etching. The ratio of spontaneous to induced tracks is proportional to the age.

Another method of determining uranium concentration is through LA-ICPMS, a technique where the crystal is hit with a laser beam and ablated, and then the material is passed through a mass spectrometer.

Applications

Unlike many other dating techniques, fission-track dating is uniquely suited for determining low-temperature thermal events using common accessory minerals over a very wide geological range (typically 0.1 Ma to 2000 Ma). Apatite, sphene, zircon, micas and volcanic glass typically contain enough uranium to be useful in dating samples of relatively young age (Mesozoic and Cenozoic) and are the materials most useful for this technique. Additionally low-uranium epidotes and garnets may be used for very old samples (Paleozoic to Precambrian). The fission-track dating technique is widely used in understanding the thermal evolution of the upper crust, especially in mountain belts. Fission tracks are preserved in a crystal when the ambient temperature of the rock falls below the annealing temperature. This annealing temperature varies from mineral to mineral and is the basis for determining low-temperature vs. time histories. While the details of closure temperatures are complicated, they are approximately 70 to 110 °C for typical apatite, c. 230 to 250 °C for zircon, and c. 300 °C for titanite.

Because heating of a sample above the annealing temperature causes the fission damage to heal or anneal, the technique is useful for dating the most recent cooling event in the history of the sample. This resetting of the clock can be used to investigate the thermal history of basin sediments, kilometer-scale exhumation caused by tectonism and erosion, low temperature metamorphic events, and geothermal vein formation. The fission track method has also been used to date archaeological sites and artifacts. It was used to confirm the potassium-argon dates for the deposits at Olduvai Gorge.

Provenance analysis of detrital grains

A number of datable minerals occur as common detrital grains in sandstones, and if the strata have not been buried too deeply, these minerals grains retain information about the source rock. Fission track analysis of these minerals provides information about the thermal evolution of the source rocks and therefore can be used to understand provenance and the evolution of mountain belts that shed the sediment. This technique of detrital analysis is most commonly applied to

zircon because it is very common and robust in the sedimentary system, and in addition it has a relatively high annealing temperature so that in many sedimentary basins the crystals are not reset by later heating.

Fission-track dating of detrital zircon is a widely applied analytical tool used to understand the tectonic evolution of source terrains that have left a long and continuous erosional record in adjacent basin strata. Early studies focused on using the cooling ages in detrital zircon from stratigraphic sequences to document the timing and rate of erosion of rocks in adjacent orogenic belts (mountain ranges). A number of recent studies have combined U/Pb and/or Helium dating (U+Th/He) on single crystals to document the specific history of individual crystals. This double-dating approach is an extremely powerful provenance tool because a nearly complete crystal history can be obtained, and therefore researchers can pinpoint specific source areas with distinct geologic histories with relative certainty. Fission-track ages on detrital zircon can be as young as 1 Ma to as old as 2000 Ma.

Fission track dating vs Radiometric K–Ar Dating

The K–Ar age of a crystalline rock represents the time since the rock last cooled below the closure temperature of potassium-bearing minerals, typically around 150–300°C, depending on the mineral. This method is useful for dating the original crystallization or significant thermal events that reset the isotopic clock.

On the other hand, the apatite fission-track age records a much lower temperature history, typically around 60–120°C. This means that while the K–Ar age reflects deeper geological processes, the apatite fission-track age captures more recent cooling and exhumation events. The difference in ages occurs because fission tracks in apatite are reset at lower temperatures, making them sensitive to near-surface thermal histories.

So, if the apatite fission-track age is considerably younger than the K–Ar age for the same rock, it suggests that the rock experienced a prolonged cooling history, possibly due to uplift and erosion bringing it closer to the surface.

Closure temperature

The closure temperature is a key concept in radiometric dating techniques. It refers to the temperature at which a mineral or rock system becomes a closed system for a specific isotopic decay process—meaning that parent and daughter isotopes no longer diffuse out of the mineral and remain locked in place. The closure temperature is important as it determines the age recorded by a dating method. The radiometric age reflects the time from when the mineral cooled below its closure temperature. Different minerals have different closure temperatures, so geologists can use multiple dating techniques to reconstruct a rock's thermal history.

Examples of closure temperatures:

Dating Method	Mineral	Closure Temperature (°C)
K-Ar dating	Biotite	~280–350
U-Pb dating	Zircon	>1000
Apatite fission-track	Apatite	~120
(U-Th)/He dating	Apatite	~70

For instance, zircon has a very high closure temperature (>1000°C), meaning its U-Pb age typically reflects the time of crystallization. In contrast, apatite fission-track dating records much lower temperatures (~120°C), making it useful for studying near-surface cooling and exhumation.

Metamorphism plays a crucial role in radiometric dating because it can reset isotopic clocks by heating and recrystallizing minerals. When a rock undergoes metamorphism, its minerals may lose their original isotopic composition due to diffusion or recrystallization, meaning that radiometric ages often reflect the time of metamorphism rather than the rock's original formation.

Metamorphic vs Intrusion Events

It is possible to mistake a metamorphic event for an intrusion event when interpreting radiometric ages, because both metamorphism and intrusion can produce new mineral growth, deformation, and chemical changes, making it challenging to differentiate them without detailed petrological and isotopic studies. For example, an intrusion into metamorphic country rock: intrusions bring heat, which can cause contact metamorphism in the surrounding rock and reset isotopic systems, making it difficult to distinguish between the age of the intrusion and the age of metamorphic country rock. Another effect is partial resetting – some minerals may retain older isotopic signatures while others reset, leading to mixed ages that can be misinterpreted.

Comparing ages from different minerals helps determine whether the event was a metamorphic overprint or an igneous intrusion.

Ophiolites and Serpentinites

Open Petrology
Free Textbook for College-Level Petrology Courses

https://opengeology.org/petrology/13-metamorphism-of-mafic-rocks/#1371

Earth's mantle is made of ultramafic rocks. Peridotites, including mostly lherzolite, harzburgite, and dunite, dominate. At mid-ocean ridges, these ultramafic rocks rise to fill space created when plates diverge. This leads to decompression melting, creating mafic magmas that crystallize in the upper part of the lithosphere as gabbros, or that erupt as seafloor basalts.
Overall, the oceanic lithosphere consists of a thin part of the uppermost mantle (ultramafic), overlain by mafic and ultramafic crust, in turn overlain by thin layers of seafloor sediments. The lithosphere cools and becomes denser during seafloor spreading, and so sinks. Thus, the youngest seafloor and highest elevations are at the ridges, and the oldest seafloor and lowest elevations at ocean margins (Figure 3.21). The oceanic lithosphere may not be the same composition and structure everywhere, but all evidence suggests that there are some standard components. The evidence comes from many sources including drill core, seismic studies, laboratory experiments, grab sampling from the ocean floor, and dredging. The best information, however, may come from studies of ophiolites. The term ophiolite derives from the Greek words ophio (snake) and lite (stone), referring to the commonly green color of the rocks that make up ophiolites.

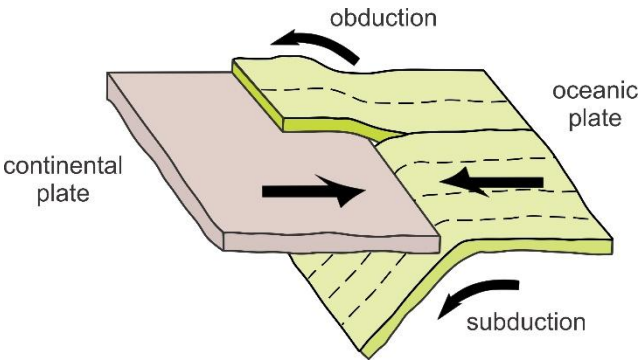

Obduction and subduction occurring at a subduction zone

Where oceanic and continental plates converge, oceanic lithosphere generally subducts beneath the continent. Sometimes, however, pieces of oceanic lithosphere are scraped off and added to a continent. We call this process obduction (Figure 13.33). Because of obduction, ultramafic rocks, formerly pieces of the mantle, can be found in ophiolite complexes. These complexes are wedges of ocean crust and mantle, now exposed in outcrops at the surface, that were thrust onto continental margins above subduction zones. Ophiolites are very important to geologists because they provide direct evidence for the nature of Earth's oceanic crust and upper mantle. Although there are many ophiolites around the world, most are small or very fragmented. Table 13.2 lists some of the best known and studied ones. Most ophiolites are 10s or 100s of millions of years old because the processes of sea-floor spreading and obduction are slow. The Macquarie Island Ophiolite, the youngest known, is still more than 10 million years old.

Every ophiolite provides a partial cross section of the oceanic lithosphere. When geologists combined information from many ophiolites with other evidence, a standardized model of the oceanic lithosphere, shown in Figure 13.34, emerged. A "complete" ophiolite would include all the layers of rock shown in the figure. These layers, which correspond to sediments and igneous rocks created by seafloor spreading, make up a cross section of the oceanic lithosphere. At its

top, muds and other debris typically overlie hard rock. These sediments, which increase in thickness from mid-ocean ridges to ocean margins, may eventually lithify to form shale or chert. A layer of basalt, often containing pillow lavas, worm-like bodies formed during submarine eruptions, underlies the sediments. These basalts, like many ocean floor basalts, are commonly highly altered by interaction with seawater.

Magmas that create ocean-floor basalts rise from magma chambers below, following fractures and creating vertical, parallel, mafic dikes. The many dikes produce a sheeted dike complex beneath the basalts. At still greater depth, a thick layer of gabbro is the remains of once liquid basaltic magma chambers (see Figure 13.34). The gabbro layer, accounting for most of the oceanic crust by volume, typically contains mafic to ultramafic cumulates in its lowest levels. Figure 13.36 is a photo of gabbro layers in the Troodos ophiolite – the browner layers contain significant amounts of orthopyroxene compared with the lighter colored layers. Peridotites (mainly harzburgites and lherzolites) of the oceanic mantle can be found beneath the gabbro layer.

13.36 Layered gabbro from the Troodos Ophiolite in Cyprus

The peridotites in the oceanic lithosphere are very high-temperature rocks and consequently the minerals they contain are unstable under normal crustal conditions. High-temperature minerals are especially unstable in the presence of water. So when uplifted to become part of the oceanic lithosphere, original olivine and pyroxenes typically are metamorphosed by seawater to produce a variety of different hydrous minerals. Further hydration also occurs during tectonism associated with subduction zones.

During continental collision and obduction, ophiolites may become incorporated into mountain belts to become bodies of rock we call alpine peridotites. These peridotite bodies range from

small slivers to large plutons. Often the peridotites are dismembered pieces – all that remain of once more complete oceanic lithosphere. Alpine peridotites typically contain serpentinized rocks.

Ophiolite emplacement

Wikipedia

There is yet no consensus on the mechanics of emplacement, the process by which oceanic crust is uplifted onto continental margins despite the relatively low density of the latter. All emplacement procedures share the same steps nonetheless: subduction initiation, thrusting of the ophiolite over a continental margin or an overriding plate at a subduction zone, and contact with air.

Scientists have drilled only about 1.5 km into the 6- to 7-kilometer-thick oceanic crust, so scientific understanding of oceanic crust comes largely from comparing ophiolite structure to seismic soundings of in situ oceanic crust. Oceanic crust generally has a layered velocity structure that implies a layered rock series similar to that listed above. But in detail there are problems, with many ophiolites exhibiting thinner accumulations of igneous rock than are inferred for oceanic crust. Another problem relating to oceanic crust and ophiolites is that the thick gabbro layer of ophiolites calls for large magma chambers beneath mid-ocean ridges. However, seismic sounding of mid-ocean ridges has revealed only a few magma chambers beneath ridges, and these are quite thin. A few deep drill holes into oceanic crust have intercepted gabbro, but it is not layered like ophiolite gabbro.

Beyond issues of layer thicknesses mentioned above, a problem arises concerning compositional differences of silica (SiO_2) and titania (TiO_2). Ophiolite basalt contents place them in the domain of subduction zones (~55% silica, <1% TiO_2), whereas mid-ocean ridge basalts typically have ~50% silica and 1.5–2.5% TiO_2. These chemical differences extend to a range of trace elements as well (that is, chemical elements occurring in amounts of 1000 ppm or less).

Additionally, the crystallization order of feldspar and pyroxene (clino- and orthopyroxene) in the gabbros is reversed, and ophiolites also appear to have a multi-phase magmatic complexity on par with subduction zones. Indeed, there is increasing evidence that most ophiolites are generated when subduction begins and thus represent fragments of fore-arc lithosphere. This led to introduction of the term "supra-subduction zone" (SSZ) ophiolite in the 1980s to acknowledge that some ophiolites are more closely related to island arcs than ocean ridges. Consequently, some of the classic ophiolite occurrences thought of as being related to seafloor spreading (Troodos in Cyprus, Semail in Oman) were found to be "SSZ" ophiolites, formed by rapid extension of fore-arc crust during subduction initiation.

A fore-arc setting for most ophiolites also solves the otherwise-perplexing problem of how oceanic lithosphere can be emplaced on top of continental crust. It appears that continental accretion sediments, if carried by the down going plate into a subduction zone, will jam it up and cause subduction to cease, resulting in the rebound of the accretionary prism with fore-arc lithosphere (ophiolite) on top of it. Ophiolites with compositions comparable with hotspot-type eruptive settings or normal mid-oceanic ridge basalt are rare, and those examples are generally strongly dismembered in subduction zone accretionary complexes.

Partial Melting and Fractional Crystallization

https://opengeology.org/petrology/03-magma/

See also Appendix of My GeoGuide No. 22: Uppermost Nappes of the Asterousia Mts - Coast Road Kali Limenes to Chrysostoms.

Just as ice melts when temperature goes above 0 ^{o}C, rocks will melt if heated to temperatures above their melting temperatures. To accomplish this rock melting requires extra heat, and that poses a problem. Where is the extra heat to come from? Although radioactive decay of potassium, uranium, thorium, or other radioactive elements may create small amounts of heat, most of Earth's heat is left over from the original time of formation. This residual heat flows from Earth's interior to dissipate at the surface, and Earth has been cooling for more than 4.5 billion years. In some places, flowing magma delivers extra heat, but the origin of the heat necessary to initially create the magma is problematic.

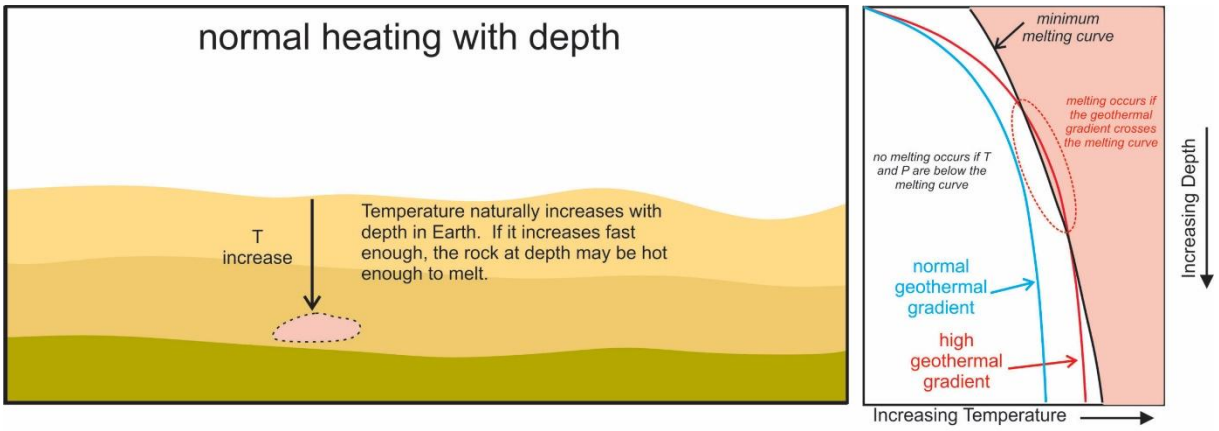

3.18 Heating with depth in Earth

Earth's average *geothermal gradient* (the rate at which temperature increases with depth in Earth) is about 25 ^{o}C/km near the surface. It is not the same everywhere – some places, such as mid-ocean ridges or hot spots like Yellowstone, have very high gradients, sometimes exceeding 50 ^{o}C/km. Other places, such as centers of old continents, have low gradients. The blue and red lines in the temperature-depth diagram on the right of Figure 3.18 are *geotherms*. The geotherms show schematically how temperature increases with depth for a place with an average gradient and for a place with a high gradient.

The solid black curve in the temperature-depth diagram of Figure 3.18 is a typical *melting curve*; it shows the minimum temperatures at which melting can occur. If temperature-depth conditions plot in the red part of the diagram, rocks will melt. The minimum melting temperature increases with depth but so do temperatures along the geotherms. In principle, if the geothermal gradient is high enough, the temperature may exceed the melting curve (shown where the red "high" geothermal gradient line crosses the black melting curve in Figure 3.18). Yet, even at mid-ocean ridges or hot spots, the gradient is generally insufficient for this to happen and cause melting. Consequently, most of Earth's mantle is unmelted.

Melting Caused by Mountain Building

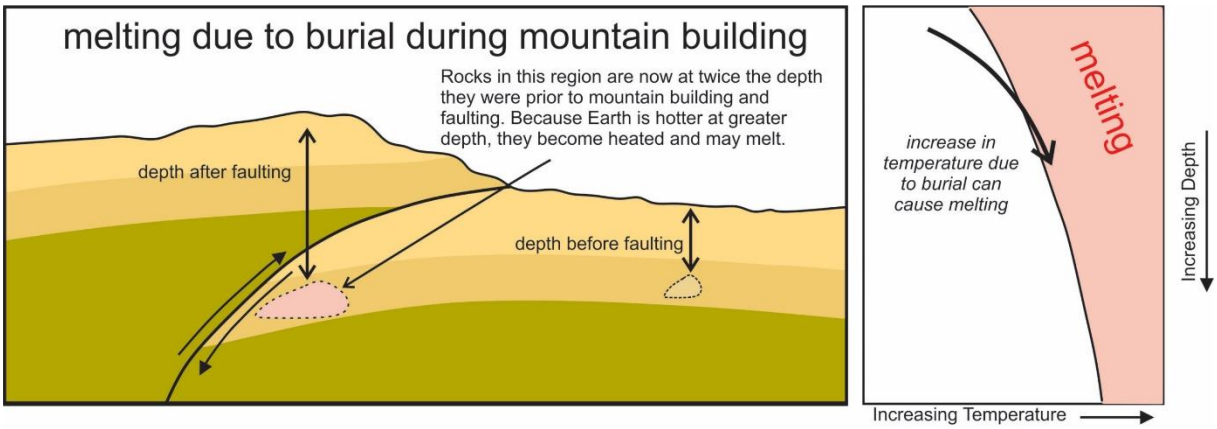

3.19 Melting during mountain building

Because a normal geothermal gradient cannot lead to melting, other mechanisms must be responsible in most cases. For instance, *tectonism* associated with mountain building can occasionally cause melting when rocks are buried by folding or faulting – because heating naturally accompanies burial (Figure 3.19). The pressure-temperature diagram on the right side of this figure shows that if burial-induced heating is great enough, melting may occur when temperatures cross into the melting field (shown in pink). Some granites in continental regions undoubtedly form by melting of sediments and sedimentary rocks, once at or near the surface, that melted after being carried to depth.

Melting Caused by Intruding Magma

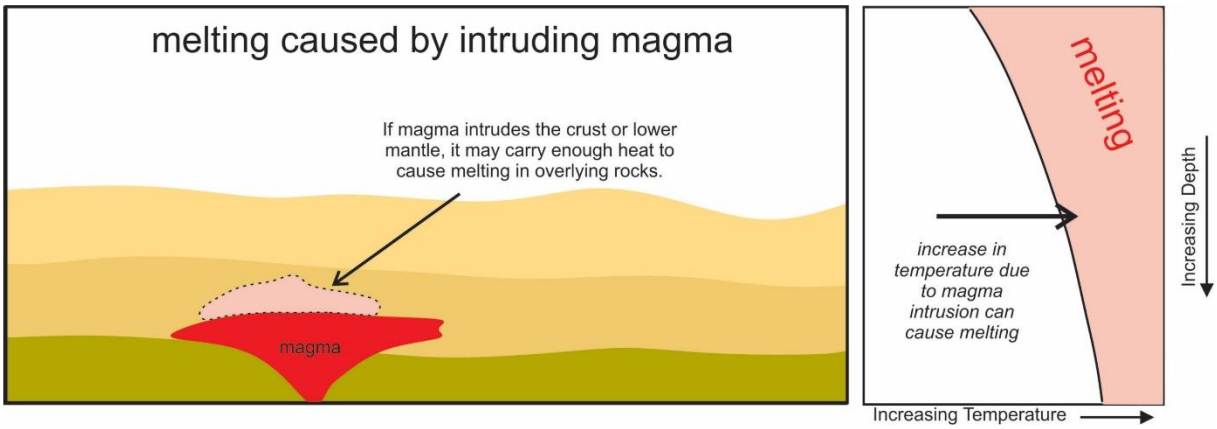

3.20 Melting caused by magmatic intrusion

Intruding magma is a very efficient mechanism for delivering heat that can cause melting (Figure 3.20). As shown by the black arrow in the pressure-temperature diagram, heat from magmas can cause temperature to increase without any increase in pressure. As discussed earlier in this chapter, beneath Yellowstone National Park, rising magmas from the mantle are hot enough to cause overlying crustal rocks to melt. In subduction zones, magmas rising above a subducting plate may cause melting in the overlying continental lithosphere, creating silicic magmas that erupt in subduction zone volcanoes or crystallize underground to become plutons.

Decompression Melting

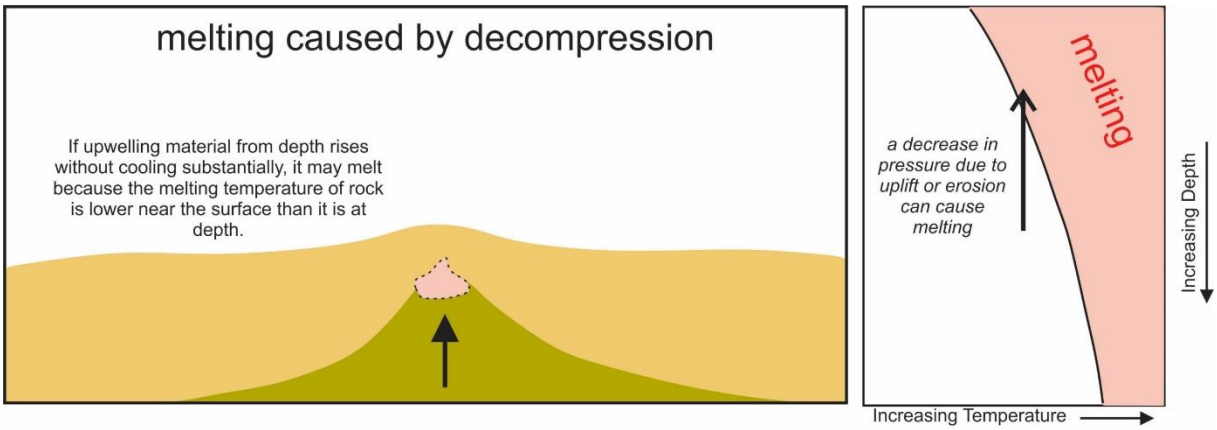

The processes described above may all cause melting, but they do not account for the widespread melting that occurs at mid-ocean ridges. There, an additional, and very significant, mechanism promotes melting – a decrease in pressure (Figure 3.21). Rising mantle moves up to fill the void created by sea floor spreading. As shown by the black arrow in the pressure-temperature diagram, the resulting pressure decrease leads to melting because rock melts at lower temperature when at low pressure, compared with high pressure. This process, called *decompression melting*, generates more magma than any other Earth process.

So, decompression melting is the key mechanism producing magmas at mid-ocean ridges, which, although we don't generally see them, are the most active volcanic settings on Earth. In these settings, partial melting of rising solid rocks produces basaltic lavas that erupt on the ocean floors, and upon cooling, are added to the spreading oceanic lithosphere. Thus the youngest oceanic crust is next to mid-ocean ridges and the oldest oceanic crust (light and dark blue) is found along ocean basin margins.

Flux Melting

Principles of thermodynamics tell us that two things combined will often melt at a lower temperature than they would individually. An analogy is a mix of ice and salt, which we all know melts at a lower temperature than ice alone. Similarly, rocks will melt at lower temperatures when they contain water, CO_2, or another volatile compared to when dry.

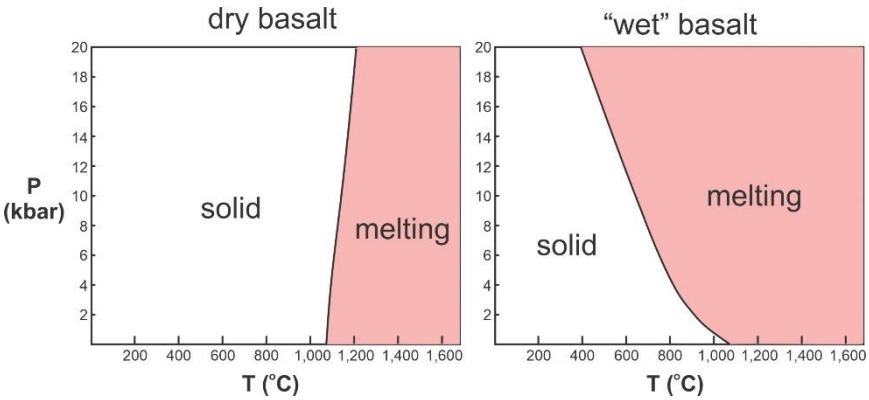

3.24 The effects of water on melting temperature of basalt

The presence of a small amount of water can change magma melting temperatures by hundreds of degrees. Figure 3.24 compares the conditions that cause melting (shown in red) of a basalt that contains no water and one saturated with a small amount of water. "Dry" basalt begins to melt at temperatures in excess of 1,000 ^{o}C. Depending on pressure, melting of "wet" basalt may begin at temperatures significantly lower. Because water and other volatiles lower melting temperatures in the same way that a *flux* is used to lower the melting temperature of metals, this additional mechanism for melting is called *flux melting*. If a rock is already hot, addition of only a small amount of water can promote melting. Water is the most important geological flux, but CO_2 and other gases also promote melting in some settings.

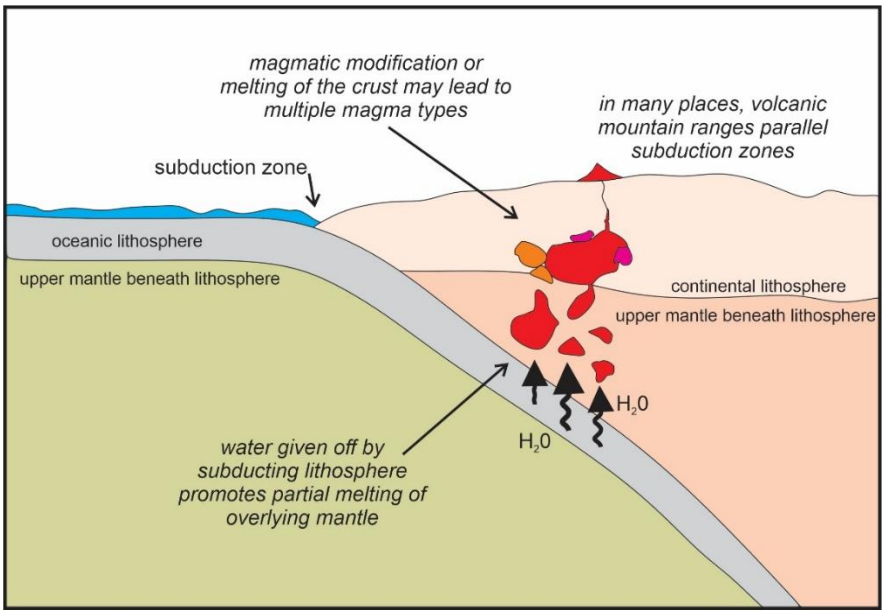

3.25 Flux melting in a subduction zone

Flux melting is especially important in subduction zones (Figure 3.25). Subducting oceanic lithosphere contains hydrous minerals that react during metamorphism to form anhydrous minerals. Consequently, water is released and migrates upwards into hot overlying mantle. This water lowers the melting temperature, causing partial melting of the ultramafic mantle to produce mafic (basaltic) magma. This magma then migrates upwards and may reach Earth's surface. It may also promote additional melting in the uppermost mantle or crust, or may become modified to produce magmas of different compositions.

Bowen's Reaction Series

When rocks melt or magmas crystallize, things are generally more complicated than when a single mineral melts or crystallizes. Most rocks contain more than one mineral, and different minerals melt or crystallize at different temperatures. N. L. Bowen, an early 20th century petrologist, conducted many laboratory experiments and was the first to compare melting and crystallization temperatures of common igneous minerals in rocks.

Bowen's Reaction Series (Figure 3.33) depicts Bowen's fundamental findings. We call it a *reaction series* because during melting (or crystallization) solid minerals continuously react with surrounding liquid.

Mafic magmas crystallize at high temperatures and felsic magmas at lower temperatures. Bowen's series shows the relative liquidus temperatures for common minerals for magmas of different compositions. As shown by the series, olivine crystallizes at the highest temperature (from mafic magmas) and quartz at the lowest temperature (from felsic magmas).

One sometimes confusing thing about this series is that it depicts liquidus temperatures for minerals when they crystallize from magmas of complex chemistry. Crystallization temperatures are different for the individual minerals if they are by themselves. For example, ignoring minor complications involving polymorphs, quartz may not begin to crystallize from a granitic melt until other minerals have formed and temperature drops to less than 1,275 ^{o}C. In contrast, quartz will crystallize from a melt of 100% SiO_2 composition at a much higher temperature (in excess of 1,700 ^{o}C).

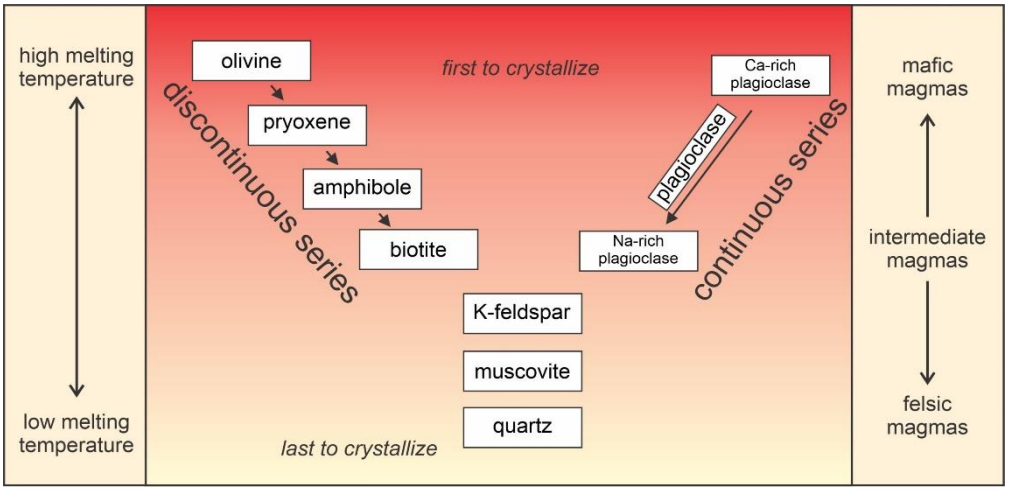

3.3 Bowen's Reaction Series

Plagioclase melts incongruently over a range of temperature depending on its composition; Bowen called the plagioclase side of the diagram the *continuous series*. Most other minerals, also depending on their compositions, melt sequentially over more restricted temperature ranges (*discontinuous series*). Bowen found that (mafic) minerals common in ultramafic and mafic rocks have the highest liquidus and solidus temperatures, and (silicic) minerals that are common in silicic rocks have the lowest. Consider a cooling magma: as temperature decreases, minerals higher up in the series crystallize first followed by minerals lower down. We call minerals that melt and crystallize at high temperatures *high-temperature minerals*; those that melt and crystallize at low temperatures are *low-temperature minerals*. The specific minerals that crystallize, however, vary with magma composition.

Although melting and crystallization in the order depicted by Bowen's Reaction Series seems straightforward, there are many complications. No magmas follow the entire series – most crystallize only one or a few of the minerals in the series – and some magmas crystallize minerals that are not part of the series. Furthermore, some minerals melt (and crystallize) congruently and some do not. Additionally, many melting and crystallization reactions involve more than one mineral reacting together. For example, at Earth's surface, anorthite melts at about 1,560 ^{o}C and diopside melts at about 1,390 ^{o}C. A rock that contains both anorthite and diopside, however, will begin to melt at around 1,270 ^{o}C, a much lower temperature than the melting point of either individual mineral.

For most magmas, crystallization begins at some maximum temperature and continues over a range of temperatures until everything is solid. As the process continues, different minerals form at different temperatures and the composition of the magma changes. The opposite occurs during heating of a rock. Melting generally begins by melting of low-temperature minerals followed sequentially by melting of higher-temperature minerals until all is liquid. During this process, the melt continually changes composition. Bowen's reaction series is a model that serves to remind us that the minerals that form depend on magma composition, that different minerals melt and crystallize at different temperatures, that mafic minerals tend to crystallize before silicic ones, and that silicic minerals melt at lower temperatures than mafic minerals do. The series does not, however, apply in detail to any known magma or rock composition. And, as pointed out above, the series only applies to rocks and magmas – it does not tell us about the melting and crystallization temperatures of individual minerals when they are by themselves.

The Importance of Partial Melting and Fractional Crystallization

Incomplete Melting

Melting can only occur if temperature exceeds the solidus, and temperatures rarely, if ever, reach the liquidus. Because the geothermal gradient is different in different places, this means that partial melting occurs but does not occur everywhere. So, magmas generally form by melting of an originally solid *parent rock* that does not melt completely. When a rock melts only partially, producing a melt that contains melted low-temperature minerals and leaving behind solid high-temperature minerals, we call the process *anatexis*. In the mantle, for example, anatexis of ultramafic rock produces basalts.

3.34 Metasedimentary migmatite

Migmatites (from the Greek *migma* meaning *mixture*, and *ite*, referring to *rock*) are rocks composed of two different components that are mixed, or swirled, together. Typically migmatites contain a light colored segregation that in many cases appears to have formed by partial melting of the darker surrounding material. In the crust, many migmatites, such as the one seen in Figure 3.34, are thought to have formed by anatexis associated with metamorphism of a parental sedimentary rock. The result is a mixed rock that contains both metamorphic and igneous components. The melt that develops eventually cools and crystallizes just like any other magma does, and will sometimes contain large crystals (phenocrysts) after completely solidified. If the melt migrates away from where it was produced, identifying its origin may become problematic, and the residual material left behind will not resemble the original

sedimentary parent. It seems apparent, nonetheless, that large scale anatexis of crustal rocks can produce large volumes of granitic melts that later form granitic plutons. The plutons may contain xenoliths (included unmelted pieces) of the original rock that melted to form the granitic magma.

Equilibrium or Not?

In an equilibrium melting process, the melt and solid remain in contact and in chemical equilibrium as melting occurs. The system is "closed" – the overall composition does not change – so the melt and remaining solid material add up to the starting composition. Consider the melting process that may occur when a rock is heated. Melting begins at the solidus temperature, and the first melt is formed by the melting of low-temperature minerals, singly or in combination. The rest of the minerals remain unmelted. Melting progresses as temperature increases, and different minerals melt at different temperatures.

As the amount of melting increases, the melt composition evolves to be more like its original parent rock until everything has melted. During this process, the minerals present will change, and the compositions of solid solution mineral crystals will change as atoms migrate in and out of the solid crystals. It does not matter if the rock melts partially or completely; if melt and solids continue to react, chemical equilibrium is possible as compositions change in response to temperature changes. The same concept of equilibrium applies to crystallization. If equilibrium is maintained during crystallization, crystals will be homogeneous in composition and will change proportions and compositions systematically as temperature decreases. However, disequilibrium can occur if the migration of atoms through the solid crystals, or through a viscous melt, is not fast enough to keep up with cooling.

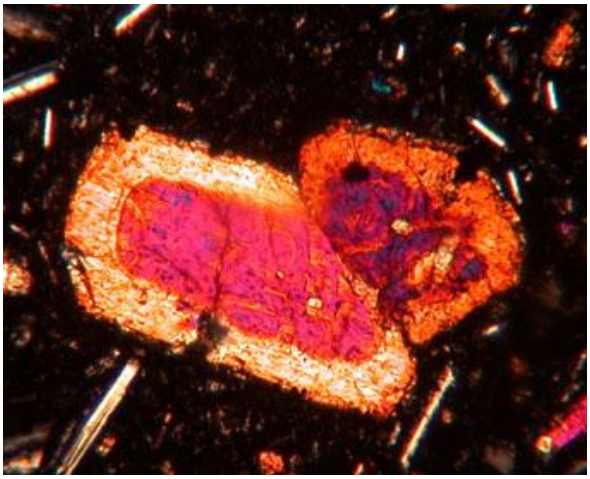

3.35 A zoned clinopyroxene crystal in a basalt

When studying rocks, petrologists may find it difficult to decide if crystals and melt stayed in equilibrium. Some volcanic rocks, however, contain zoned crystals that are evidence of disequilibrium. We saw two examples in Figure 3.31. Figure 3.35 is another example. It shows a polarizing microscope view of a large compositionally zoned grain of clinopyroxene in a basalt. The dark material surrounding the clinopyroxene is mostly volcanic glass, and the needle-shaped light colored crystals are plagioclase. If the clinopyroxene grain was homogeneous, the colors induced by the polarizers would be the same in all parts of the grain. Zoning of this sort is evidence that the melt and crystals did not stay in equilibrium during crystallization. Figure 3.31 shows similar zoning in plagioclase. In both cases, the centers of

the crystals grew at high temperature, and as temperature decreased the crystals grew larger. If the minerals and melt stayed in equilibrium, the grain (no matter the size) would have a homogeneous composition. But in zoned crystals the crystal cores have compositions formed at higher temperature than the rims did. The outer zones have compositions that formed at lower temperature because atoms could not migrate into and through the crystals fast enough to maintain compositional homogeneity. Thus, only partial equilibrium was maintained. Many volcanic mineral crystals have broad homogeneous centers but are zoned near their rims, suggesting that they stayed in equilibrium with the melt until the latest stages of crystallization.

Partial Melting

Large scale disequilibrium melting occurs if a melt and a solid do not continue to react together, but instead become chemically isolated due to physical separation. For example, if a rock melts partially and the magma escapes upwards, the melt and remaining solid material cannot react to stay in chemical equilibrium.

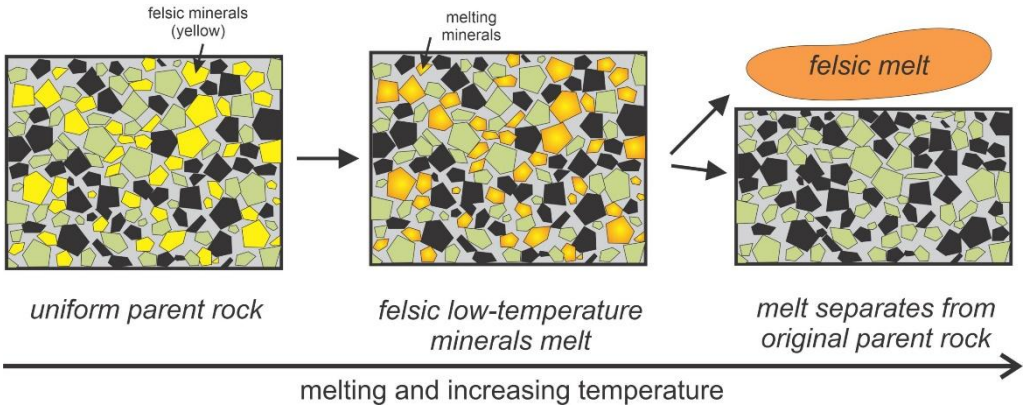

3.36 Partial melting

Figure 3.36 shows melting of an original parent rock that contains several different minerals. The first minerals to melt are (generally Si-rich) low-temperature minerals (shown in yellow). So, initial melting produces a relatively silicic magma (shown in orange). This melt may subsequently become separated from the leftovers of the original rock. Consequently, a melt of different composition from the parent has been produced and may move upwards in Earth.

Partial melting is a widespread and important process that occurs in the source region for most magmas. Low-temperature minerals always melt first, either individually or in consort with others. They are relatively silica-rich minerals compared with others in a rock, so when partial melting occurs, the melts are more silicic than the parent rock is. The remaining rock becomes depleted in silicic components and, therefore, more mafic than its parent. When this happens, silicic melts migrate upwards, leaving more mafic residue behind. So, partial melting explains, in part, why the Earth has differentiated into a more silicic crust and more mafic mantle during its 4.6 billion year lifetime. These generalizations always apply, but the specific products of partial melting depend on the starting material composition and the amount of melting. Furthermore, the results will be different if the parent rock is already depleted.

Earth's mantle is ultramafic; if it melted completely it would produce ultramafic magma, but, as discussed previously, complete melting cannot occur because there is no known mechanism for heating the mantle to the very high temperatures needed to melt it completely. Partial melting, however, is common, and the upper mantle is the source of many magmas that move

within the crust and sometimes reach the surface. Because the upper mantle has a relatively uniform composition, partial melting of mantle produces similar magmas worldwide, almost all mafic, equivalent to basalt compositions. More silicic magmas may also be generated in the mantle, but they are uncommon. Similarly, partial melting of subducted ocean crust, which is basaltic everywhere, generally produces magmas of intermediate composition, and partial melting of lower continental crust produces silicic magmas (equivalent to granite).

Fractional Crystallization

Fractional crystallization, the opposite of partial melting, occurs when a magma partially crystallizes and the remaining magma becomes segregated from the crystals. In these circumstances, the new *evolved magma* will have a different composition from its *parental magma*. The evolved magma, which is more silicic than its parent was, may move upwards, leaving the high-temperature (mafic) minerals behind. Fractional crystallization, like partial melting, has been a key process contributing to differentiation of Earth.

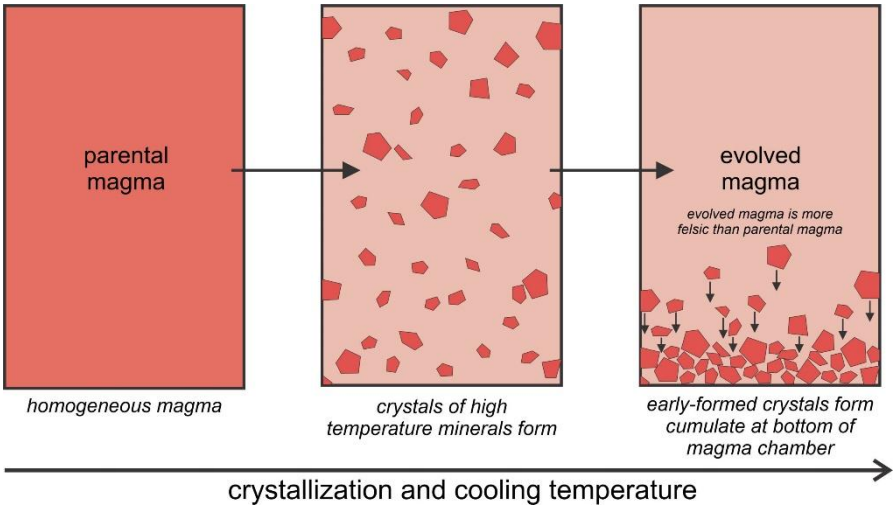

3.37 Diagram showing fractional crystallization

Fractional crystallization may occur when newly formed crystals sink to the bottom of a magma chamber and no longer stay in equilibrium with the melt. Figure 3.37, a schematic diagram, shows the principles involved. While cooling, a parental magma crystallizes some high temperature minerals. These minerals eventually sink to the bottom of the magma chamber, leaving an evolved magma above. Because high-temperature minerals are mafic, the evolved melt is more silicic (less mafic) than the original parent magma. During this process, a *cumulate* rock forms at the bottom of the magma chamber, and the evolved magma may move upwards and become completely separated from the cumulate. Fractional crystallization explains the origins of cumulate rocks like the chromite cumulates.

Other Processes Explaining Variations in Magma Composition

Fractional crystallization is undoubtedly the most important process that changes magma composition after a magma forms. Other mechanisms, however, also lead to changes. For example, in some settings, hot magmas may melt surrounding rocks and assimilate them into the magma. Generally, we think of this *assimilation* occurring when mafic magmas encounter more silicic rocks, because mafic magmas may be hotter than the silicic rock's melting temperature is. So, assimilation can make magma more silicic and is most likely to occur in the

(silicic) crust. Some volcanic rocks contain crustal xenoliths, inclusions of rock fragments incorporated as solid pieces into the melt; often the xenoliths show evidence of partial melting. It is no stretch to assume that sometimes xenoliths melt and mix in completely. Some geochemical data, too, supports the idea that crustal material has been incorporated into a mantle-derived melt.

Different magmas may also combine to produce hybrid magmas of different compositions. However, *magma mixing* is unlikely to happen if magma compositions are too different because different magmas have different melting temperatures, densities, and viscosities. Although some evidence suggests that magma mixing occurs on a small scale, most petrologists believe it is generally a minor contributor to magma diversity. A third process, *liquid immiscibility*, has also been proposed as a process that may lead to change in magma composition. Immiscible liquids unmix in much the same way that chicken soup separates into broth and fat upon cooling. Experimental evidence suggests, for instance, that sometimes a sulfide-rich melt may unmix from mafic silicate magma – a potential important process forming ore deposits, or that alkali-rich magmas may unmix from less alkaline ones.

Parental Magmas and Differentiation

Only a few rare magmas may not be evolved. For example, the white veins (termed *leucosomes*) in migmatites that form by partial melting of sedimentary rocks may not have changed composition after they formed (Figure 3.34). The leucosomes appear to have been created by partial melting of metasedimentary rock, and the melt has remained local and has not differentiated.

The majority of magmas, however, evolve from some parental magma. They are evolved melts, not melts having the composition created during initial melting. Subsequently, as crystallization progresses, magma compositions follow what is called a *liquid line of descent,* producing a series of magmas of different compositions as fractional crystallization removes specific minerals from the melt.

If solid mantle melted directly, either partially or completely, to create magma, the magma would be called a *primary magma*. Primary magmas have undergone no differentiation and have the same composition they started with. Specifically, if they come from the ultramafic mantle, and were not subsequently modified, they must have a very high Mg:Fe ratio and be enriched in Cr and Ni just like mantle rocks, and petrologists use these and other characteristics to test if magmas could be primary magmas. Most magmas fail the tests, and primary magmas are exceptionally rare, or may not exist at all. Some magmas and rocks, however, come close to being primary, and petrologists describe them as *primitive,* meaning they have undergone only minor differentiation.

Parental magmas may be primary or primitive. The only requirement is that they lead to magmas of other compositions. If a collection of melts with different compositions evolve from the same parent, they form a *magma series*. Although the melts have different compositions, they will share some chemical characteristics, especially trace element compositions and isotopic ratios. A challenge for petrologists is to study the compositions of an inferred magma series to learn the composition and source of the original parent.

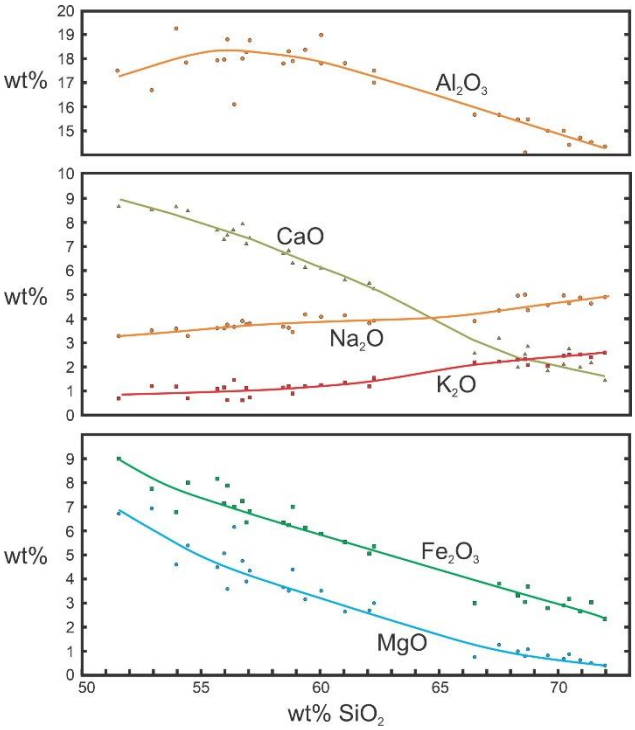

3.40 Harker diagram for volcanic rocks of the Crater Lake region, Oregon

Typically, petrologists begin their quest by obtaining analyses of the rocks and plotting the results on different kinds of *composition diagrams*. For example, *Harker diagrams*, first used in 1902, have SiO2 content as the horizontal axis and other oxides plotted vertically (Figure 3.40). SiO2 is chosen as the abscissa because it generally shows the most variation of all oxides, and because it relates closely with magma temperature and the amount of fractional crystallization.

When looking at Harker diagrams, the principles are that (1) if derived from a common parent, rock compositions should trend smoothly across a diagram; and (2) the most mafic composition is closest to the parent magma composition. So, if a Harker diagram reveals smooth trends, it is possible that all the magmas derived from the same parent and that the low SiO2 end of the graphs are closest to the magma's parent composition. Harker diagrams are only one kind of composition diagram; many others with different oxides on the axes are commonly used.

Figure 3.40 shows a well-studied Harker diagram for volcanic rocks from near Crater Lake, Oregon, based on the data of Howell Williams (1942). Each point represents a different volcanic rock from the same region; the horizontal axis shows the SiO2 content of the rock and the vertical axis the amount of other oxides present. The solid lines show the smoothed trends. The smooth trends are evidence that the different rocks may have derived from the same original parental magma. The Crater Lake magmas range from *basalt* (on the left side of the diagram) to *rhyolite* (on the right side). Based on the trends shown, Williams concluded that the magmas all came from a common parent magma and that they evolved by fractional crystallization. The basalt composition is closest to that parent.

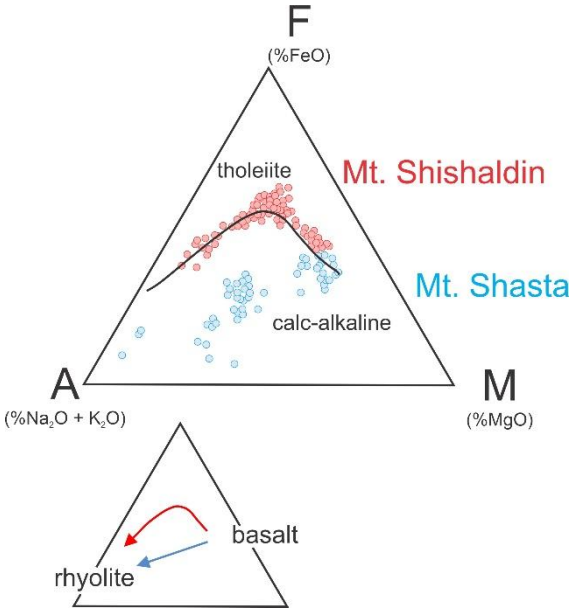

3.41 AFM diagrams for rocks from Mt. Shishaldin, Alaska, and from Mt. Shasta, California

A second commonly used way to look at magma composition is to plot compositions on an AFM diagram (Figure 3.41). AFM diagrams ignore SiO2 and instead look at alkali (Na2O + K2O), iron as FeO (assuming it is not Fe2O3), and MgO content. The triangle corners are: A = alkali oxide weight %, F = FeO weight %, and M = MgO weight %. Many studies have found that magma series follow one of two trends, the *tholeiite* trend or the *calc-alkaline* trend, and we easily see these on an AFM diagram. Figure 3.41 is an AFM diagram comparing rocks from Shishaldin Volcano (Aleutian Islands) and Shasta Volcano (California). Each point represents an analysis of an individual rock. Shishaldin is an island arc volcano associated with an oceanic plate subducting under another oceanic plate. Shasta is a continental margin volcano where an oceanic plate is subducting under a continental plate. The Shishaldin data follow a tholeiite trend, depicted by the solid line and red arrow that initially moves toward the F-corner before curving downward toward the A-corner. The Shasta data follow a calc-alkaline trend (depicted by the blue line that heads directly toward the A-corner).

Whether tholeiitic or calc-alkaline, originally mafic magmas can produce rocks ranging from basalt to rhyolite, as the bottom triangle in Figure 3.41 shows. At both Shishaldin and Shasta Volcanos, more primitive parental magmas were mafic and the later evolved magmas were silicic. They differ, however, because tholeiitic magmas become iron-rich as they evolve, moving initially toward the F apex of the triangle. Calc-alkaline trends go directly from basalt to rhyolite.

The trends on an AFM diagram reveal clues about the environments in which the magmas differentiated. The difference between calc-alkaline and tholeiite trends is due to the oxidation state of iron. If iron is mostly oxidized, magnetite (Fe3O4), a mineral that contains oxidized iron (Fe3+), crystallizes early from a melt. If the iron is mostly reduced (existing as Fe2+), magnetite does not crystallize. In calc-alkaline magmas, the iron is oxidized, leading to crystallization of magnetite. Consequently, when mafic minerals crystallize, iron is removed from the magma as fast as magnesium and the melt's Fe:Mg ratio remains about constant during differentiation. In tholeiitic magmas, olivine and pyroxene crystallize first and magnetite may not crystallize at all. Olivine and pyroxene have high Mg/Fe ratios compared with melt, and the magma becomes enriched in iron during the initial stages of crystallization. Calc-alkaline magmas are dominant in *andesitic-type* subduction zones, such as California's Cascade

Mountains. Mt. Shasta is an example. Tholeiitic trends occur mostly in island arcs, such as the Aleutian Islands, and Shishaldin Volcano is an example.

A Closer Look at Magma Chemistry

Major and Minor Elements

Major elements, typically present at levels exceeding 1 weight %, determine most magma properties and eventually the minerals that may form. Typical major elements in igneous rocks include O, Si, Al, Fe, Ca, Na, K, and Mg. In some rocks, Ti, Mn, P, and perhaps others may be considered major elements. Rocks also contain *minor elements*. Minor elements, typically comprising 0.1 to 1 weight % of a magma or rock, substitute for major elements in minerals but are selective about which minerals they enter. For the most part, they do not affect magma properties.

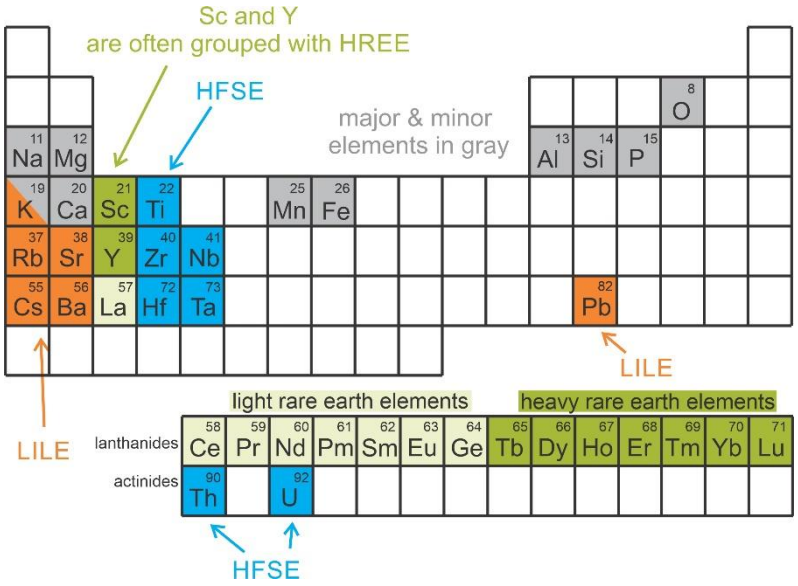

3.42 Periodic chart showing some key elements in igneous rocks

Figure 3.42 shows some key elements in igneous rocks. Major and minor elements are shaded gray. The other shaded elements are *incompatible elements* in mafic minerals (discussed in detail below). The incompatible elements include large ion lithophile elements (LILE) shaded orange, heavy rare earth and related elements shaded dark green, light rare earth elements shaded light green, and high field strength elements (HFSE) shaded blue. Potassium (K) is considered both a major element and an LILE element.

Trace elements are elements present in very small amounts, amounts even smaller than amounts of minor elements. The amount of any trace element that can enter a growing crystal depends mostly on ionic charge and radius. Some trace elements enter growing crystals in the early stages of crystallization, but others may remain in a magma until the latest stages of crystallization. Trace elements are even more selective than minor elements about the minerals they enter and generally have insignificant effects on rock and mineral properties. Because trace elements are present in very small amounts, petrologists commonly report them in parts per million (ppm) or parts per billion (ppb) instead of weight % (wt %). 1 ppm = 0.0001 wt %.

Furthermore, when plotting trace element analyses, petrologists normalize the raw data by dividing by the composition of some reference standard. Normalization means that the range of values becomes small enough so that we may plot all trace elements on a single graph.

*Table 3.3 Analysis of a Hawaiian Basalt**

major and minor elements		trace elements	
element	wt%	element	ppm
O	44.66	V	292.00
Si	23.27	Cr	238.00
Fe	8.59	Zr	129.90
Ca	8.28	Sr	129.10
Al	7.20	Ni	102.60
Mg	4.27	Zn	85.40
Na	1.81	Cu	63.30
Ti	1.64	Y	40.60
K	0.46	Ba	18.40
Mn	0.13	Ce	8.30
P	0.11	Nb	4.30
		Rb	1.30
Total	100.42	Total	1113.20

**Data are from Duncan, et al. (1990)*

Table 3.3 contains an analysis for a Hawaiian basalt.

The analysis does not distinguish between major and minor elements (because the distinction between the two is a fuzzy one), but Mn and P together comprise only about 0.2 weight % of the rock and would be considered minor elements by most petrologists. K, too, might be considered a minor element in this rock. The analysts listed trace elements separately, reporting them in ppm instead of weight %, and the total of the trace elements is about 1,113 ppm, which is equivalent to 0.1113 weight %. Many other trace elements are undoubtedly present in the Hawaiian basalt, but were not analyzed because they were not important to the study being conducted. Although Mn and P are minor elements in the Hawaiian basalt (and most other basalts), they may be concentrated in other kinds of rocks. The alkalis, major elements in silicic rocks, may be nearly absent in mafic rocks, although in the Hawaiian basalt they add to about 2.25 weight %. So, minor elements in some types of rocks can be major elements in others and vice versa.

We can classify and name igneous rocks based on the minerals they contain, but magmas, because they contain no minerals, must be classified in another way. Additionally, many volcanic rocks may contain glass instead of minerals or may be too fine grained for mineral identification. Thus we often classify magmas and many igneous rocks based on their chemical composition instead of their mineralogy.

Although igneous rock chemistry varies in many ways, the silica content and alkali content of volcanic rocks form the basis for one of the most commonly used classification schemes. It is not that other compositional variations are unimportant, but that many other possible variations correlate with alkali and silica content and so the classification system captures well the variation in rock compositions.

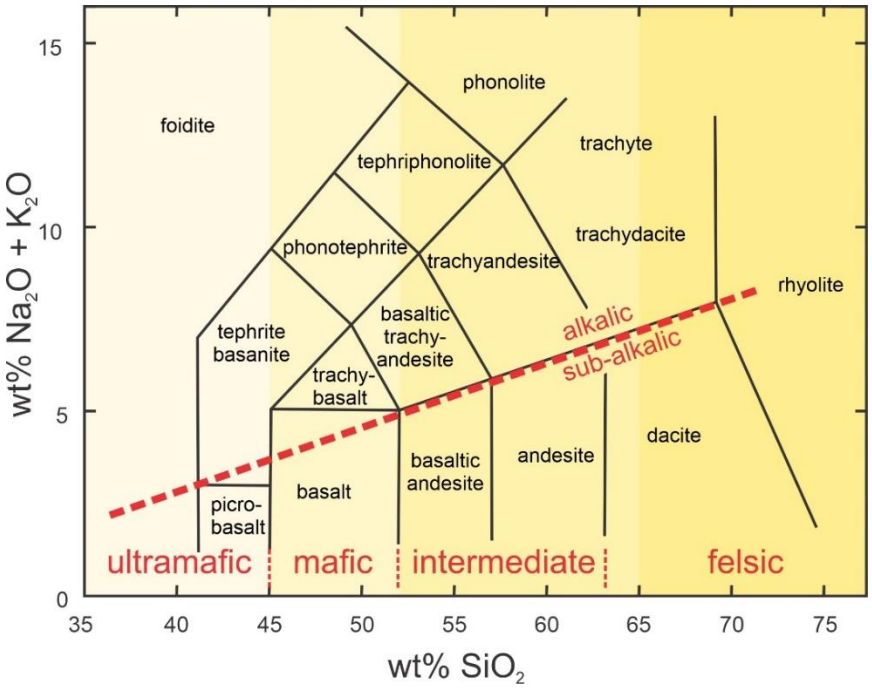

3.43 The total-alkali-silica (TAS) classification system

Using the *total alkalis versus silica* (TAS) system (Figure 3.43) is straightforward, and the weight percentages of silica (SiO_2) and alkali oxides ($Na_2O + K_2O$) in a rock are used to obtain a rock name. The vertical axis is the total alkali oxide content, and the horizontal axis is the silica content. In the TAS diagram, ultramafic compositions (low silica content) plot on the left and silicic compositions (high silica content) on the right, with mafic and intermediate compositions between. The diagonal red line divides the diagram into two parts. Compositions that plot in the upper part of the diagram are *alkalic*; they are relatively rare in nature. Those plotting in the lower part of the diagram are termed *sub-alkalic* and are much more common. By far, the most common volcanic rocks are sub-alkalic: basalt, andesite, dacite, and rhyolite. Although the names in Figure 3.43 are names of volcanic rocks, they are often used to describe magma types. A dacite magma, for example, is one that could erupt to form a dacitic rock.

Although both silica and alkali content are keys when classifying magmas or volcanic rocks, silica content alone explains many variations in magma properties (Table 3.4). It is also the basis for a rock-naming scheme that is simpler than the TAS system is: simply calling rocks ultramafic, mafic, intermediate, or silicic. Variations in magma properties with silica content are profound. The more silicic a magma, the lower its eruption temperature but the greater the possibility for explosive eruptions due to high viscosity and gas content. Note that in this simpler classification scheme, alkali content correlates with silica content. This correlation is not always the case, as shown in the TAS diagram, but is the case for sub-alkalic rocks. Similar to the names in the TAS system, the rock names in Table 3.4 are often used to describe magma composition. For example, we might describe a magma as granitic if it could crystallize to form a granite.

Table 3.4 Properties of Different Kinds of Magmas

magma type	ultramafic	mafic	intermediate	felsic
extrusive rock name	komatiite	basalt	andesite	rhyolite
intrusive rock name	peridotite	gabbro	diorite	granite
silica content (wt% SiO_2)	40-45	←	→	71-75
mafic content (wt% FeO + MgO)	high	←	→	low
ratio alkali earth/alkali (wt% $CaO/Na_2O + K_2O$)	high	←	→	low
eruption temperature	up to 1,500 °C	←	→	800 °C or less
viscosity	low	←	→	high

Incompatible and Compatible Elements

We can divide elements in igneous rocks and magmas into two groups: those that tend to remain in a magma until the later stages of crystallization (and consequently become enriched in the magma as crystallization takes place), and those that are easily incorporated into early growing crystals (and consequently become depleted in a magma quickly). Elements that tend to remain in the magma are said to be *incompatible*, and those that enter crystals quickly are *compatible*. Petrologists use these terms, incompatible and compatible, most commonly to describe trace elements, but they apply equally well to major and minor elements. Some elements behave as compatible elements in some magma types, but incompatible in others, because the specific minerals that crystallize vary with magma composition. Trace elements, however, both compatible and incompatible, are especially useful as trackers of magma evolution. Incompatible elements include the rare earth elements, elements 57 through 71 (La – Lu), but their degree of incompatibility varies with atomic number. The rare earths, and other incompatible elements are highlighted in the periodic chart of Figure 3.42.

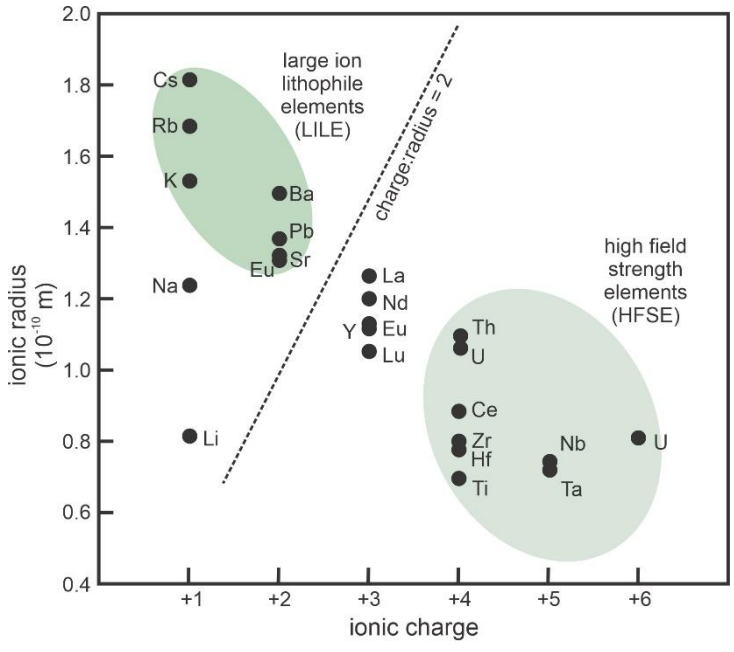

3.44 The two groups of incompatible elements

Incompatible elements fall into two main groups, a group that has large ionic radius, and a group that has large ionic charge (Figure 3.44). The first group includes alkali and alkali earth elements, notably K, Rb, Cs, Sr, Ba, and several other elements. Elements that tend to concentrate in Earth's crust and mantle are called *lithophiles*. So, the alkalis and alkali earths, and elements with similar properties, are collectively termed *large ion lithophiles*, or *LILE* for short (Figure 3.44). LILEs do not fit into crystallographic sites in most minerals, and the charge attracting them to growing crystals is small, so they tend to remain in a melt.

Elements that form ions with small radii and high charge are called *high field strength elements (HFSE)* (Figure 3.44). This group of incompatible elements includes Zr, Nb, Hf, Th, U, and Ta. HFSEs have high ionic charge (+4 or greater), which means that, if they enter crystals charge balance is hard to obtain. Consequently, HFSEs tend to remain in a melt. For some purposes, HFSE are defined as those whose ions have a charge to radius ratio greater than 2 (to the right of the dashed line in Figure 3.44).

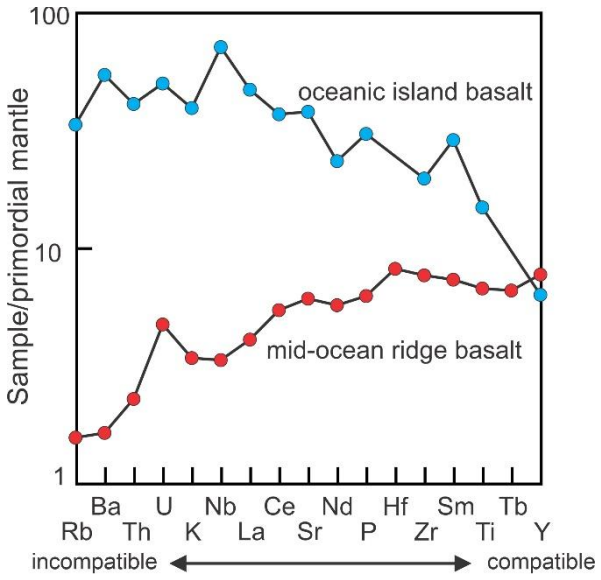

3.45 Comparing the trace element chemistry of an oceanic island basalt with a mid-ocean ridge basalt

Figure 3.45 compares the trace element content of an oceanic island basalt with that of a mid-ocean ridge basalt. In diagrams of this sort – sometimes called *spider diagrams* – the most incompatible elements are on the left, and elements are increasingly less incompatible moving to the right. The mid-ocean ridge basalt is depleted in incompatible elements compared with the oceanic island basalt. However, both have about the same concentrations of the compatible elements. This diagram, therefore, suggests that mid-ocean ridge magmas, associated with active plate spreading centers, derive from regions that have undergone significant amounts of partial melting. In contrast, the oceanic island magmas come from regions that are more primitive.

Evidence of this sort allows petrologists to conclude that the upper oceanic mantle – the source region for mid-ocean ridge basalts – is an area of active melting and recycling of material. The source of oceanic island basalts, such as those that reach the surface in Hawaii, is deeper in the mantle where melting has not removed incompatible elements. Note that the data for both

basalts were normalized by dividing the analyses by an estimated composition for the primordial mantle (to keep numbers on scale). Additionally, the vertical scale is a log scale; if it were not, the trends would not be as easily seen.

Some transition elements – including nickel, cobalt, chromium, and scandium – are also important trace elements. They have small radii, and (usually) +2 or +3 ionic charge, and are incorporated into mafic minerals during the earliest stages of crystallization and tend to remain there. So, they are compatible when melting occurs in the mantle and, consequently, melts from the mantle contain them in very low amounts. They are often used as markers that determine where in Earth a magma originated.

The concept of compatible versus incompatible elements depends on rock type, because different rocks contain different minerals that incorporate elements in different ways. Scandium may enter pyroxenes, but not enter olivine. Zirconium is easily accommodated in zircon. Phosphorus concentrates in apatite, but neither zirconium nor phosphorous go into olivine. Earth's mantle is primarily composed of olivine and pyroxene, and these minerals become enriched in scandium, nickel, titanium, chromium, and cobalt as fractional melting occurs. So, melts derived from the upper mantle are enriched in these elements, and the amount of melting that has occurred can be estimated based on trace element abundance.

Rare Earth Elements

The *lanthanide elements*, also called the *rare earth elements* (REE), having atomic numbers 57 (La) to 72 (Lu), are very important trace elements with high field strength (Figure 3.44). Elements 57 through 64, La through Gd, are considered *light REEs;* 65-71, Tb through Lu, are heavy REEs. Y and Sc are sometimes grouped with the *heavy REEs* due to similar properties. The REEs all have a large ionic radius and, except Eu, they are trivalent (+3). Ionic radius decreases with increasing atomic number, so La and other light REEs (largest) are more incompatible than Lu and other heavy REEs (smallest) are. If garnet crystallizes, it incorporates heavy REEs (Ho-Lu) easily, making them especially compatible.

During fractional crystallization of a magma in the mantle or the crust, incompatible elements stay preferentially in melts and, so, tend to move up and concentrate in Earth's outer layers. The original source region is *fertile* if there has been little removal of incompatible elements, but fertile rocks become *depleted* rocks when melting occurs. Rocks or magmas that are rich, or only slightly depleted, in light rare earth elements are fertile, and those with strong depletions in LREE are depleted, because their chemistry indicates the degree to which they have melted. This is why trace elements are powerful indicators of magma origin. Magmas that originate in upper levels of Earth are richer in incompatible elements than those that come from pristine mantle sources. Additionally, petrologists distinguish both fertile and depleted magma source regions within the mantle.

When a rock melts, the incompatible elements enter the melt quickly. Consequently, the concentration of incompatible elements will be very high after just a little bit of melting. With more melting, the concentrations decrease because most incompatible elements are already in the melt and get diluted with further melting. This effect is especially true for elements present in rocks and magma in very small amounts, which explains why trace elements are such powerful indicators of magma origin. So, trace elements tell us how much melting has occurred to produce a magma and, although a bit more complicated, they also monitor how much crystal fraction occurs when a magma cools.

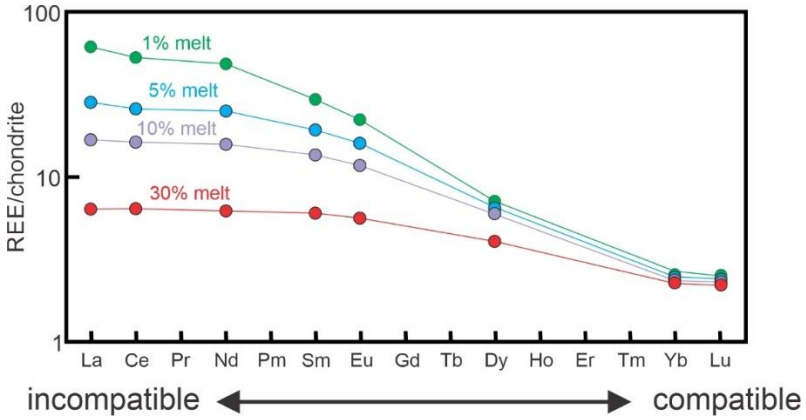

3.46 Calculated rare earth concentrations for melts derived from a garnet peridotite

Figure 3.46 shows rare earth patterns for melts derived from a garnet peridotite. If only a small amount of melting occurs, concentrations of incompatible elements are high because they enter the melt first. With increased melting, other elements enter the melt and the concentrations of incompatible elements goes down. In this diagram, the compositions were normalized by dividing by the standard composition of a chondritic meteorite, and the scale is a log scale.

Uranium–lead dating

Uranium–lead dating - Wikipedia

Uranium–lead dating, abbreviated U–Pb dating, is one of the oldest and most refined of the radiometric dating schemes. It can be used to date rocks that formed and crystallised from about 1 million years to over 4.5 billion years ago with routine precisions in the 0.1–1 percent range.

The method is usually applied to zircon. This mineral incorporates uranium and thorium atoms into its crystal structure, but strongly rejects lead when forming. As a result, newly-formed zircon crystals will contain no lead, meaning that any lead found in the mineral is radiogenic. Since the exact rate at which uranium decays into lead is known, the current ratio of lead to uranium in a sample of the mineral can be used to reliably determine its age. The method relies on two separate decay chains, the uranium series from 238U to 206Pb, with a half-life of 4.47 billion years and the actinium series from 235U to 207Pb, with a half-life of 710 million years.

Decay routes

Uranium decays to lead via a series of alpha and beta decays, in which 238U and its daughter nuclides undergo a total of eight alpha and six beta decays, whereas 235U and its daughters only experience seven alpha and four beta decays. The existence of two 'parallel' uranium–lead decay routes (238U to 206Pb and 235U to 207Pb) leads to multiple feasible dating techniques within the overall U–Pb system. The term U–Pb dating normally implies the coupled use of both decay schemes in the 'concordia diagram' (see below). However, use of a single decay scheme (usually 238U to 206Pb) leads to the U–Pb isochron dating method, analogous to the rubidium–strontium dating method.

Finally, ages can also be determined from the U–Pb system by analysis of Pb isotope ratios alone. This is termed the lead–lead dating method. Clair Cameron Patterson, an American geochemist who pioneered studies of uranium–lead radiometric dating methods, used it to obtain one of the earliest estimates of the age of the Earth.

Mineralogy

Although zircon ($ZrSiO_4$) is most commonly used, other minerals such as monazite (see: monazite geochronology), titanite, and baddeleyite can also be used. Where crystals such as zircon with uranium and thorium inclusions cannot be obtained, uranium–lead dating techniques have also been applied to other minerals such as calcite / aragonite and other carbonate minerals. These types of minerals often produce lower-precision ages than igneous and metamorphic minerals traditionally used for age dating, but are more commonly available in the geologic record.

Mechanism

During the alpha decay steps, the zircon crystal experiences radiation damage, associated with each alpha decay. This damage is most concentrated around the parent isotope (U and Th), expelling the daughter isotope (Pb) from its original position in the zircon lattice. In areas with

a high concentration of the parent isotope, damage to the crystal lattice is quite extensive, and will often interconnect to form a network of radiation damaged areas. Fission tracks and micro-cracks within the crystal will further extend this radiation damage network. These fission tracks act as conduits deep within the crystal, providing a method of transport to facilitate the leaching of lead isotopes from the zircon crystal.

Computation

Under conditions where no lead loss or gain from the outside environment has occurred, the age of the zircon can be calculated by assuming exponential decay of uranium. That is

$$N_{\mathrm{n}} = N_{\mathrm{o}} e^{-\lambda t}$$

where

- $N_{\mathrm{n}} = \mathrm{U}$ is the number of uranium atoms measured now.
- N_{o} is the number of uranium atoms originally - equal to the sum of uranium and lead atoms $\mathrm{U} + \mathrm{Pb}$ measured now.
- $\lambda = \lambda_{\mathrm{U}}$ is the decay rate of Uranium.
- t is the age of the zircon, which one wants to determine.

This gives

$$\mathrm{U} = (\mathrm{U} + \mathrm{Pb})\, e^{-\lambda_{\mathrm{U}} t},$$

which can be written as

$$\frac{\mathrm{Pb}}{\mathrm{U}} = e^{\lambda_{\mathrm{U}} t} - 1.$$

The more commonly used decay chains of Uranium and Lead gives the following equations:

$$\frac{^{206}\mathrm{Pb}^*}{^{238}\mathrm{U}} = e^{\lambda_{238} t} - 1, \qquad \textbf{(1)}$$

$$\frac{^{207}\mathrm{Pb}^*}{^{235}\mathrm{U}} = e^{\lambda_{235} t} - 1. \qquad \textbf{(2)}$$

(The notation Pb ∗ Pb*, sometimes used in this context, refers to radiogenic lead. For zircon, the original lead content can be assumed to be zero, and the notation can be ignored.) These are said to yield concordant ages (t from each equation 1 and 2). It is these concordant ages, plotted over a series of time intervals, that result in the concordant line.

Loss (leakage) of lead from the sample will result in a discrepancy in the ages determined by each decay scheme. This effect is referred to as discordance and is demonstrated in Figure 1. If a series of zircon samples has lost different amounts of lead, the samples generate a discordant line. The upper intercept of the concordia and the discordia line will reflect the original age of formation, while the lower intercept will reflect the age of the event that led to open system behavior and therefore the lead loss; although there has been some disagreement regarding the meaning of the lower intercept ages. *[Wikipedia]*